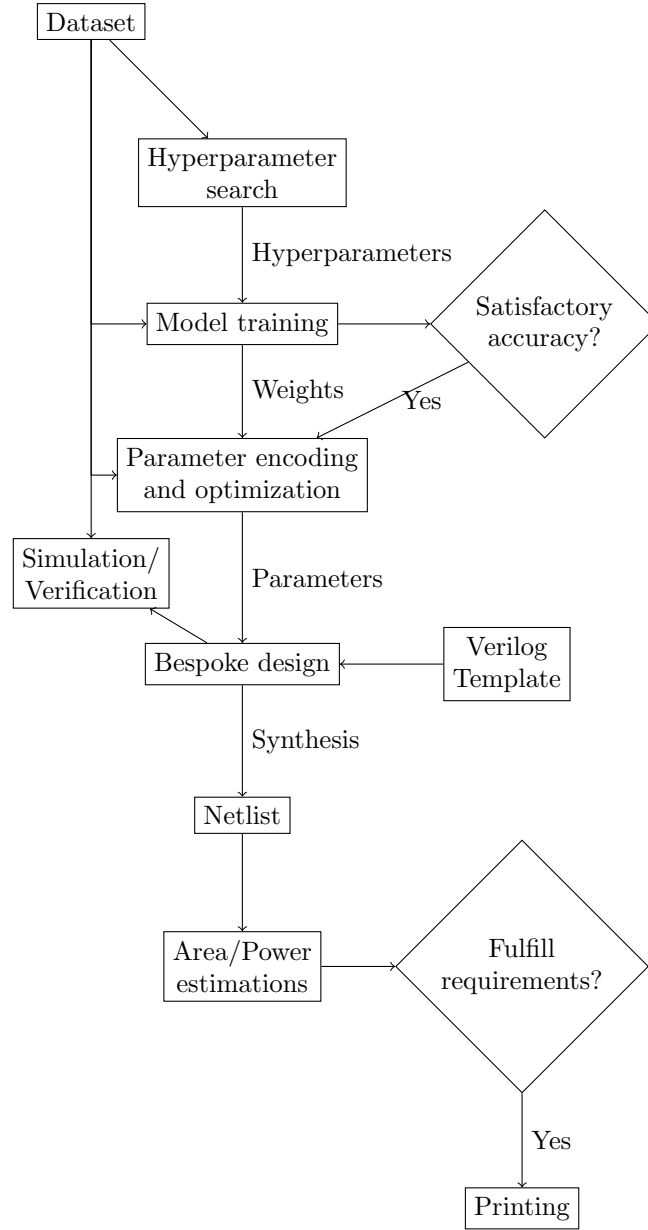# Contents

1 Proposed framework

Figure 1: Proposed framework

As outlined in the ubiquitous computing section, the deliverable of this thesis is meant to be a framework that allows a labeled set of sensor data to produce a fully

functional printed circuit that implements a classifier for this dataset. Due to lack of access to equipment the actual printing is not viable in this context and the scope will be restricted to the dataset to netlist part of the process.

The classifier architecture will in particular be a Binary Neural Network(BNN), explained in the preliminaries. It may not necessarily be the most suitable architecture in every case, but it was created with the purpose to reduce resource consumption, which is the core concern. It was thus chosen as the niche I will be carving here.

The rough sequence of processes performing that transformation comprises of the following:

1. Hyperparameter search: In order for a hands-off training process to be applicable to a vast space of possible sensor datasets for which printed classifiers may be desired a single generic configuration of training hyperparameters wont cut it. So a search must be performed to find a set suitable to the data distribution at hand.
2. Model training: After a useable hyperparameter configuration is found a model is trained under them and evaluated. If the test split accuracy is sufficient for the user's needs the rest of the process may take place. The weights and network architecture of the final model are passed to be processed.
3. Parameter optimization: Some pieces of information derived from the weights and dataset can be used to help the design avoid unnecessary computations. For an extreme but applied example, if a neuron never changes it's output based on its input activations it can be flagged to be replaced with a static constant assignment.
4. Parameter encoding: The weights, measures of the network architecture and derived assisting information are either used to produce verilog code that performs the computations they imply or formatted such that they can be read and parsed by the control mechanisms of verilog.
5. Design instantiation: A template for the type of design that ought to be produced gets the snippets of custom functionality and/or the formatted parameters needed to derive that functionality using generate blocks imported into it. The result is a design that is bespoke to the exact trained model under question.
6. Verification: A behavioural simulation of the design is performed to confirm that classifier accuracy is satisfactorily preserved.
7. Synthesis: An optimised netlist is produced from the HDL specification. A farther gate level simulation is performed to guarantee functionality.
8. Metric estimation: Area and power estimates are taken from the synthesis

and simulation tools using information from the printed components PDK. If these demands seem to be supported by the budget of the usecase the user may place a printing order.

Parts of the wider procedure out of scope of this framework are:

- Printed sensor availability
- Access to printed sensor data for labeling
- Examination of other promising architectures
- Design of masks for placement of printed components
- Inclusion of sensor, ADC and output indicator resource consumption in reported estimates.

The rest of the thesis will almost entirely deal with the design of efficient bespoke BNN classifier hardware. This includes parts 3 and 5 of the process listed above. The rest, although time consuming to implement, have no parts of interest to report on and will be summarised in the experimental setup section.

The points that I think are helpful to be impressed upfront in order for my following talk of HDL implementations to be comprehensible are:

- Over the course of working on the presented designs 6 models that correspond to 6 of the 7 datasets shown above are consistently used to test and compare results. The one dataset of the 7 that didn't make the cut was Arrhythmia, because the learned strategy of the model wasn't acceptable.

- All of these networks have one hidden layer that takes 4 bit inputs that are received from the ADCs connected to the respective sensors and one output layer that receives 1 bit binary inputs from the previous layer and produces a score for how likely each class is. An argmax module is also included in all of the following implementations to provide the index of the predicted class and is also included in the area/power estimates.

- All these networks have exactly 40 hidden neurons in the first layer. This is not reflective of an actual limitation of the framework. A first batch of models that were used to evaluate the designs and were meant to be replaced at some point ended up staying until the end. Initially they were kept out of inertia and past some point replacing them would require re-evaluating every type of design implementation with every new model in order for result comparisons to be informative, which would take a substantial usage of synthesis time and would halt further progress for a while.

- During synthesis a practically unlimited timing budget is allowed so timing optimizations do not take place and trade off against more important to the

project goals.

- The power draw estimate is done with a gate level simulation of the synthesised circuit evaluating 1000 samples of the dataset to reproduce a realistic usage environment. The clock frequency is set to the critical timing frequency of the circuit reported by the synthesis tool.

1.1 Symbol definitions

- N = the number of input features,

- M = the number of hidden neurons (in our case it is always 40),

- C = the number of output neurons/ number of classes

- S be the number of samples in the dataset,
- x_i be the ith input feature,

- x_i be the i-th input feature,

- D^i be the i-th sample of the dataset,
- D_j^i be the value the j-th input feature takes on the i-th sample of the dataset,
- h_i be the i-th hidden neuron, also used to denote it's output value before binarization,

- s_i be the i-th hidden neuron's output after binarization, so $s_i = h_i \geq 0$,

- y_i be the i-th output neuron, also used to denote it's output value,

- $W1$ = the weight matrix of the first layer,

- $W2$ = the weight matrix of the second layer,

Rows represent neurons and columns represent input activations, so $W1_{i,j}$ is the weight of the first layer that corresponds to the connection between the input feature x_j and the neuron h_i.

2 Fully combinatorial fully connected implementations

Two initial approaches for implementing the fully connected BNNs in a fully combinatorial single-cycle datapath are compared. Only the first layer differs between them, the second layer stays unchanged.

2.1 Positive-Negative Sum
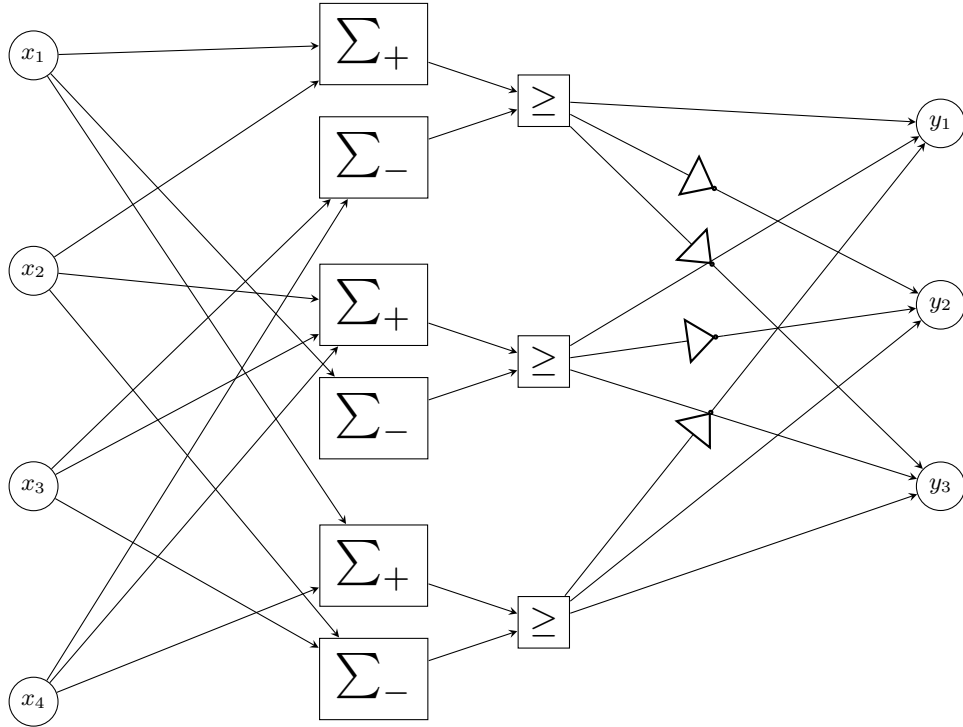
Figure 2: Implementation with positive and negative sums split

For each neuron in the first layer two sums are calculated. Σ_i^+ is the sum of the input features for which the connection with the i-th hidden neuron has a positive weight , whereas Σ_i^- the sum of those that have a negative weight associated. The two sums are then compared and if the positive sum is greater than or equal to the negative the output of the neuron is 1, otherwise 0.

$$\Sigma_i^+ = \sum_{j=0}^{N-1} x_j [W1_{i,j} > 0]$$

$$\Sigma_i^- = \sum_{j=0}^{N-1} x_j [W1_{i,j} < 0]$$

$$h_i = \Sigma_i^+ \geq \Sigma_i^-$$

Sample code snippet:

```
assign positives[0] = + feature_array[1] + feature_array[2] +
↳   ... + feature_array[10];
assign negatives[0] = + feature_array[0] + feature_array[3] +
↳   feature_array[5];
assign hidden[0] = positives[0] >= negatives[0];
```

The reasoning behind splitting the sums is that keeping the operations to only using unsigned positive numbers and only using addition and not subtraction means simpler operations are required, and that may lead to a smaller footprint.

For each neuron of the output layer it's value is calculated by summing the output of hidden neurons. The binary output of the hidden neuron s_j is added as-is to the sum of the output neuron y_i in the case that the weight of their connection $W2_{i,j}$ is positive and it's binary inverse is added to the sum if $W2_{i,j}$ is negative. This is equivalant to the sum of the xnor between the output vector of the hidden layer and the weight vector of the output neuron.

$$y_i = \sum_{j=0}^{M-1} \begin{cases} s_j, & \text{if } W2_{i,j} > 0 \\ \neg s_j, & \text{if } W2_{i,j} < 0 \end{cases}$$

Code sample:

```
assign scores[0*SUM_BITS+:SUM_BITS] = + hidden_n[0] + hidden[1]
↳   + hidden[2] + ... + hidden_n[39];
```

2.2 Signed sum
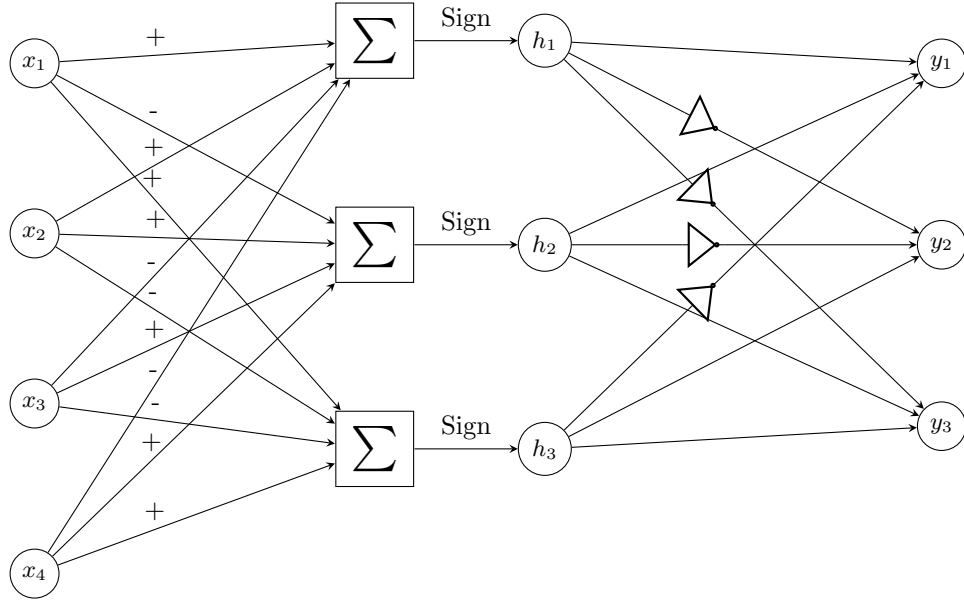
Figure 3: Implementation a single sum per neuron

In this version a single sum is calculated for each neuron. If the connection between input feature x_j and hidden neuron h_i has weight $W1_{i,j} = 1$ it is added to the sum, otherwise it is subtracted from it. Basically adding the feature multiplied by either 1 or -1 is hard-coded as the resulting addition or subtraction correspondingly. The result is then compared to zero to give the binarized output of the neuron. Since the result is a signed number, this just means taking the sign bit.

$$h_i = \sum_{j=0}^{N-1} \begin{cases} +x_j, & \text{if } W1_{i,j} > 0 \\ -x_j, & \text{if } W1_{i,j} < 0 \end{cases}$$

Code sample:

```
wire signed [8:0] intra_0;
assign intra_0 = - feature_array[0] + feature_array[1] + ... +
↪   feature_array[10];
assign hidden[0] = intra_0 >= 0;
```

The second layer's implementation is not changed from how it is described above.

2.2.1 Results and analysis

Table 1: Comparison of single signed sum to double unsigned sums approaches

	bnnpar area(cm²)	bnnparsign area(cm²)	area change	bnnpar power(mW)	bnnparsign power(mW)	power change
Har	29.4	24.52	-16.6%	92.1	78.8	-14.4%
cardio	46.71	33.27	-28.8%	145.3	106.2	-26.9%
gasId	269.76	175.09	-35.1%	767.7	499.1	-35.0%
pendigits	42.95	33.38	-22.3%	136.8	108.9	-20.4%
winered	27.82	22.45	-19.3%	90.7	74.6	-17.8%
winewhite	26.01	20.47	-21.3%	84.6	68	-19.6%
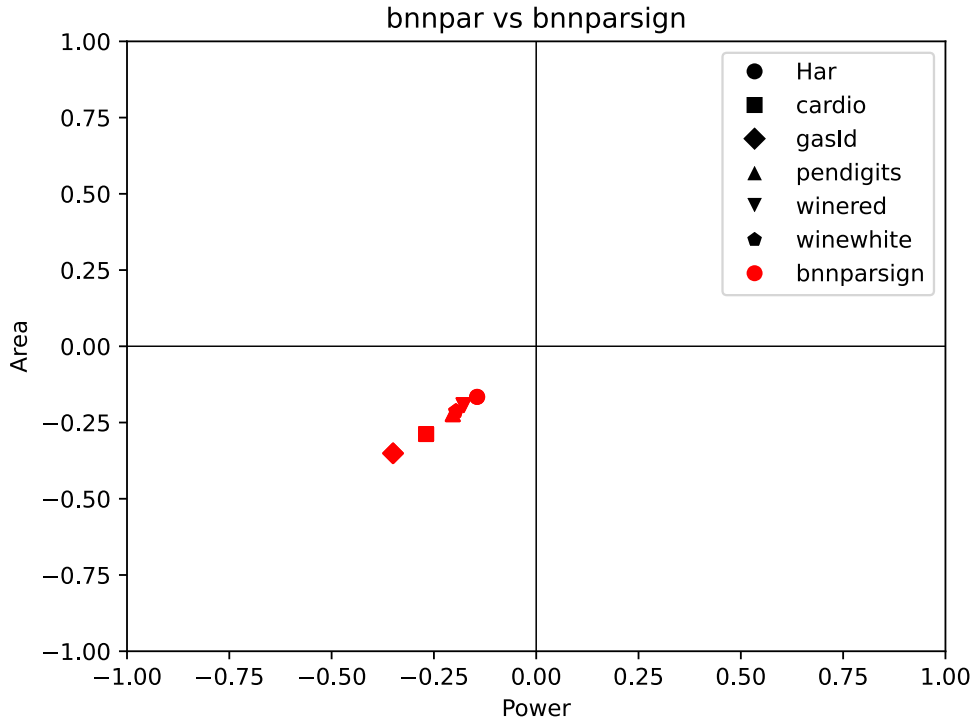
Figure 4: Comparison of single signed sum to double unsigned sums approaches

My prior expectation was that splitting the features into two sums to avoid subtractions would lead to better results than keeping all the operations for a neuron to a single expression by the reasoning summarised previously. In fact it turns out that using a single sum has area and power requirements 20-30% lower than using two.

My explanation for this is that keeping terms in separate expressions prevents the compiler from effectively locating and reducing shared subexpressions during synthesis. For example, if a neuron's expression contains $+x_5 + x_6 - x_7$ and a different neuron contains $-x_5 + x_6 + x_7$ then the result of $x_5 - x_7$ can be used for both neurons, but if x_5 and x_7 are not in the same expression, as they would not be in the positive-negative sum implementation, this arithmetic optimization is not used by the compiler. Additionally the two sums need comparators to produce the binarized output of the neuron, whereas in the case the signed sum this corresponds to the sign bit of the sum which means no additional hardware.

2.3 Minimum range bit-width reduction
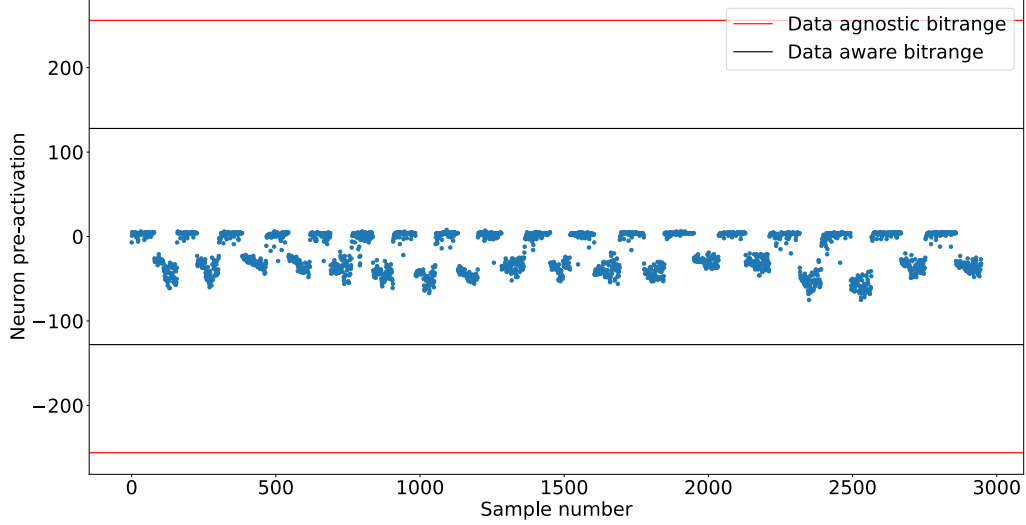
Figure 5: Pre-activation values for a hidden neuron for each sample of the dataset and comparison of the default and minimum bitrange that supports all values.

The reasoning goes that if the bitwidth that is demanded for the total sum of the features is reduced, the bitwidth that partial sums it depends on require lower on the adder graph is also reduced. As a consequence, adders need to accomodate less bits and less logic ought to be implemented for them.

At least in theory, the minimal circuit to implement the calculations of the sums of the first layer with reduced widths for the results should be strictly equal or smaller than the one with full widths. This is because given a circuit that implements the full width calculations, the reduced width results can be taken by selecting the bitrange of that width from the least significant bits of the full width result. This is simple wire selection and does not require any additional hardware, therefore reducing neuron widths can never require additional logic.

So far in the first layer the bitwidth of the total sum h_i of the neuron is set to be large enough to fit any value that may come up as the result of M additions and subtractions of 4-bit unsigned numbers. The assumption is that this range is significantly wider than the range of values the neuron actually takes during evaluation of typical samples. This would mean the bitwidth can be lowered without errors due

13

to overflows or underflows coming up in actual use of the design, and this lowering would improve performance.

To test this the total sum of each neuron h_i is calculated for each sample in the dataset. I get the minimum and maximum of these values. Since all values for the total sum to take are contained in the range between those two, the arithmetic operations need not accomodate any range larger than that. Let H_j^i be the value of h_i when evaluating the i-th sample of the dataset, and wh_i be the bitwidth of the i-th hidden neuron.

$$h_{imax} = \max_{j=0}^{S-1} H_j^i$$

$$h_{imin} = \min_{j=0}^{S-1} H_j^i$$

$$wh_i = \lceil \log_2(\max(h_{imax}, |h_{imin}| - 1)) \rceil + 1$$

2.3.1   Results and analysis

Table 2: Results of restricting neuron bitwidths

	bnnparsign area(cm²)	bnnparw area(cm²)	area change	bnnparsign power(mW)	bnnparw power(mW)	power change
Har	24.52	24.25	-1.1%	78.8	77.6	-1.5%
cardio	33.27	33.21	-0.2%	106.2	105.4	-0.8%
gasId	175.09	171.37	-2.1%	499.1	486.9	-2.4%
pendigits	33.38	33.97	+1.8%	108.9	109.6	+0.6%
winered	22.45	21.87	-2.6%	74.6	72.3	-3.1%
winewhite	20.47	20.36	-0.5%	68	66.7	-1.9%
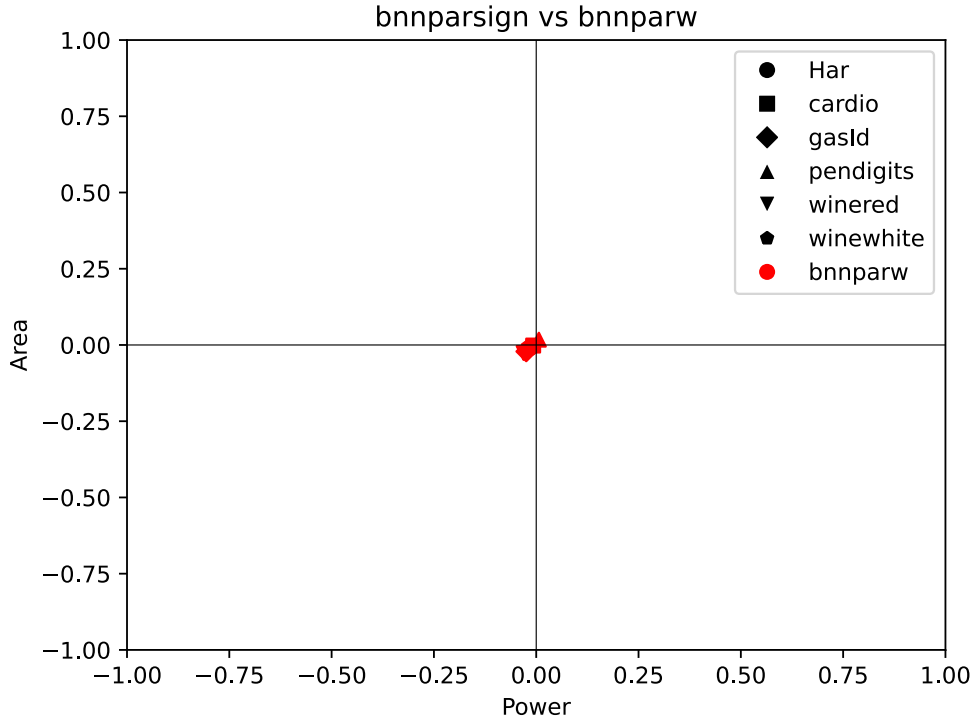
Figure 6: Results of restricting neuron bitwidths

The results are negligible, in the 1-3% range, and in the case of pendigits they even deteriorate a bit. This deterioration should not be possible in theory if the synthesised circuits are optimal implementations of their description. This is at least evidence that the negligible results on the other datasets can be better if I can get them into a form the compiler can work better with, though I still think the main problem is with the approach itself. It seems that the truncation goes against best practices and blocks the datapath extraction process for some neurons, so certain optimizations do not get applied to them and some would be common resources do not get shared. I have not found a method to work around this limitation at this point.

2.4 Naively reducing bitwidths of intermediate results

2.4.1 Rationale

Given the eventual goal of applying approximate computation techniques to the adder graph of the designs a problem, mentioned previously, comes up. If the approximation, whatever it may be, gets applied separately to each neuron's sum, almost certainly blocks the datapath extraction process from performing arithmetic optimizations such as reducing and sharing common subexpressions across neurons. The result is M separate approximate adder trees. Even given that the logic reduction gained from approximate additions for each adder tree is more than enough to offset the lost benefit of intermediate result sharing, that may be an unnecessary concession.

To estimate how large the negative effect of an approximation technique not taking cross-neuron sharing into consideration could be, I reduce the bitwidths of intermediate results of the sum of each neuron. Even though this would reasonably help for a single neuron, I expect it will cause resource sharing to break. Given how large the negative effect is I can check if this is a problem than ought to be fixed before approximation can confidently be applied.

2.4.2 Implementation
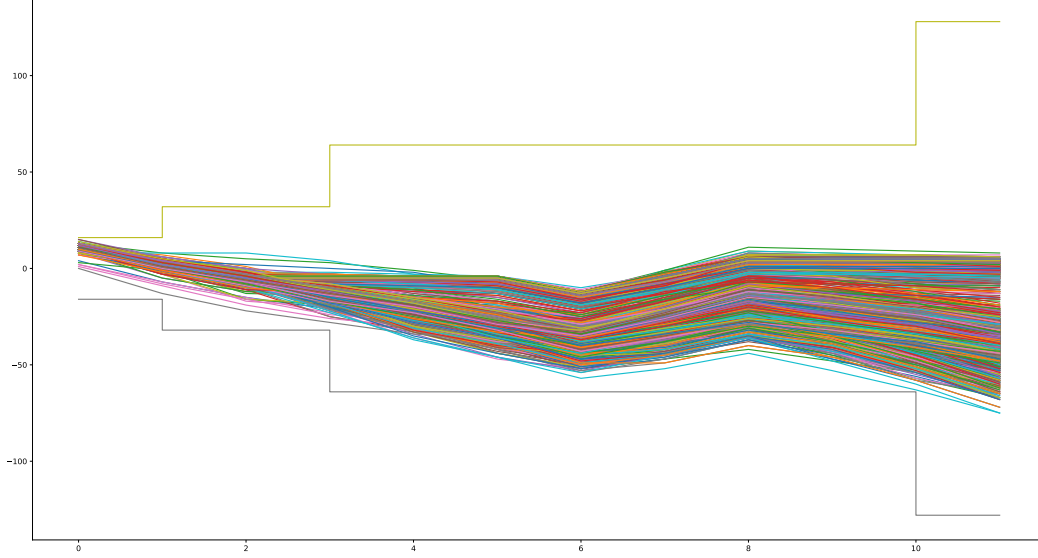
Figure 7: The intermediate sums of the sequential calculation of hidden neuron 28 for all of the Har dataset and the bit range needed to support each step

The cumulative sum along the input features multiplied by the weight of their connection with the neuron i is calculated for each hidden neuron and for each sample of the dataset. The maximum and minimum values over all samples at each step of the cumulative sum for a given neuron is then calculated. In a similar fashion to the method described above for reducing the bitwidth of the total result of the neuron's operations, the operations are written sequentially with the result of each having it's bitwidth set based on the range of values for the equivalent step of the sum for all of the dataset.

Let $h_{i,j}$ denote the result of the pre-activation value of the i-th hidden neuron only taking into account the input features x_0 to x_j, or equivalently the value of h_i if x_{j+1} to x_{N-1} are masked to zero.

$$h_{i,j} = \sum_{k=0}^{j} x_k W1_{i,k}$$

$$hmax_{i,j} = \max_{l=0}^{S-1} \sum_{k=0}^{j} D_k^l W1_{i,k}$$

$$hmin_{i,j} = \min_{l=0}^{S-1} \sum_{k=0}^{j} D_k^l W1_{i,k}$$

$$wh_{i,j} = \lceil \log_2(\max(hmax_{i,j}, |hmin_{i,j}| - 1)) \rceil + 1$$

Sometimes due to the order of additions and subtractions the width needed at a later step is less than the one of an earlier step. This is because every sample for which there would be an overflow in the earlier step with the smaller width would at some following feature underflow back in the range it supports. This has been taken into account. If a width of a subsequent operation's result is smaller, the bitwidth of the previous addition/subtraction is simply set to that smaller value.

$$wh'_{i,j} = \min_{k=j}^{N-1} wh_{i,j}$$

Consecutive operations that have the same result bitwidth are grouped together and expressed in verilog as a single sum. I have not confirmed if this does in fact affect the result of synthesis at all but it seems to conform closer to the recommendations of the best practices guide.

2.4.3   Results and analysis

Table 3: Results of shrinking intermediate results naively

	bnnparw area(cm²)	bnnparstepw area(cm²)	area change	bnnparw power(mW)	bnnparstepw power(mW)	power change
Har	24.25	23.16	-4.5%	77.6	73.7	-5.0%
cardio	33.21	39.29	+18.3%	105.4	125.5	+19.1%
gasId	171.37	326.98	+90.8%	486.9	935.2	+92.1%
pendigits	33.97	37.09	+9.2%	109.6	120.3	+9.8%
winered	21.87	22.78	+4.2%	72.3	75.3	+4.1%
winewhite	20.36	20	-1.8%	66.7	65.8	-1.3%
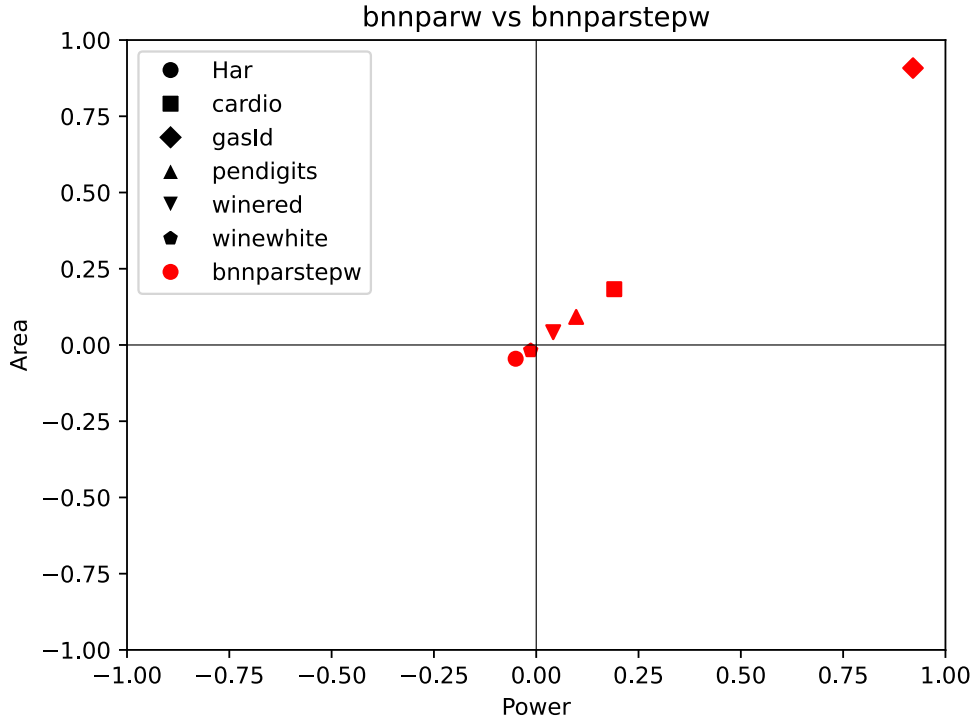
Figure 8: Results of shrinking intermediate results naively

The results were positive for two of the models with the smallest count of input features N, which means that this method performed better than the initial expectation. However, the optimization loss from losing shared operations shows clear scaling with the number N of input features. With more elements to sum, more common subexpressions to optimise ought to come up, so this is keeping with expectations.

At the network with the largest N, the one belonging to gasId, which has 128 sensor features, it has gotten bad enough to almost double the area and power requirements. This shows that the issue is indeed considerable when there is more than a handful of inputs, and ways to work around it shall be searched for.

2.5 Preemptive arithmetic optimization
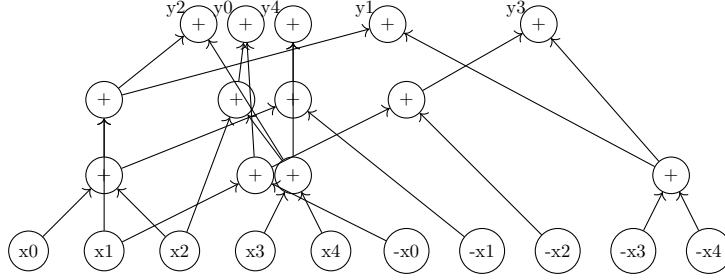
Figure 9: Implementation of a binary weight layer with a preconfigured order of additions.

2.5.1 Rationale

Based on the results from above I attempt to get the arithmetic expression that the design computes after synthesis, with the intent of fitting later approximation techniques to it rather than having the approximations dictate the graph of operations and forego these advantages.

Design compiler provides an "*resource and datapath extraction*" report, which quoting the user guide "analyzes the arithmetic contents of the design and provides feedback so you can improve the RTL code as needed". In this report the arithmetic operations that are performed post-optimization by each datapath block are described in the block's resource section. From this an addition / subtraction graph from input elements to layer outputs could be reconstructed with relatively straightforward parsing.

Unfortunately, the report does not provide a mapping between the symbols it uses for input and output variables of the datapath blocks and the corresponding wires in the original design. Due to this the reconstructed adder graph cannot be used to implement the network's layers before the inputs and outputs are otherwise labeled.

Conceivably a method that unfolds all intermediate steps of the calculation into full explicit sums of input variables for each output variable could be used to achieve this labeling. After all intemediate variables / nodes of the adder graph are eliminated (for example, $x = a + b; y_1 = c + x; y_2 = d - x;$ would be expanded to $y_1 = c + a + b; y_2 = d - a - b;$) the addition and subtraction operations can be mapped to a matrix with binary {-1, 1} weights. A permutation matrix that turns the original weight matrix of the layer into this reconstructed matrix is then searched for, and

20

the permutations are assigned as the labels of the input and output elements of the adder graph.

Another path around this problem comes from the inclusion of references to the operator or operators in the original verilog design that is implemented by a given arithmetic operation mentioned in a datapath block's report. These references only point to the line of the verilog file the operator apears in, so to narrow it down with certainty the HDL file must beformated in a way that only a single arithmetic operator occurs per line.Then the variables named as operants in the report can be matched to the variables associated with the operator in the line or lines pointed to.

Some early attempts in this direction are made but it becomes clear that a process that involves the network to be implemented in an HDL, synthesized, reverse engineered from the synthesised result, implemented in HDL in a different way and re-synthesised would require considerably more complex orchestration than first impressions imply. Even if it panned out without any issues the speed with which modifications to the designs could be tried out would be slowed down to a degree I was not comfortable with.

As an alternative I search the literature for algorithms or heuristics that would perform an equivalent arithmetic optimization to the one Design Compiler provides. It does not appear too hopeful that a de facto standard method for such cases exists and perhaps even is the one used under the compiler's hood, so the operations found are exactly or close to the same.

Var	Type	Data Class	Width	
I1	PI	Unsigned	4	
I2	PI	Unsigned	4	
I3	PI	Unsigned	4	
I4	PI	Unsigned	4	
I5	PI	Unsigned	4	
I6	PI	Unsigned	4	
I7	PI	Unsigned	4	
I8	PI	Unsigned	4	
I9	PI	Unsigned	4	
I10	PI	Unsigned	4	
I11	PI	Unsigned	4	
I12	PI	Unsigned	8	
I13	PI	Unsigned	7	
I14	PI	Unsigned	8	
T1540	IFO	Unsigned	5	I5 + I6 (winered_bnn1_bnnpar.v:44winered_bnn1_bnnpar.v:48winered_bnn1_bnnpar.v
T1848	IFO	Unsigned	6	I4 + T1540 (winered_bnn1_bnnpar.v:80winered_bnn1_bnnpar.v:99winered_bnn1_bnn
T1994	IFO	Unsigned	5	I11 + I8 (winered_bnn1_bnnpar.v:48winered_bnn1_bnnpar.v:51winered_bnn1_bnnpar
T1567	IFO	Unsigned	5	I10 + I7 (winered_bnn1_bnnpar.v:40winered_bnn1_bnnpar.v:44winered_bnn1_bnnpar.v:48wine
T1548	IFO	Unsigned	6	I9 + T1567 (winered_bnn1_bnnpar.v:40winered_bnn1_bnnpar.v:44winered_bnn1_bnn
T2045	IFO	Unsigned	7	T1994 + T1548 (winered_bnn1_bnnpar.v:48winered_bnn1_bnnpar.v:75winered_bnn1_
T2042	IFO	Unsigned	8	I3 + T1848 + T2045 (winered_bnn1_bnnpar.v:99)
T158	IFO	Unsigned	5	I1 + I2 (winered_bnn1_bnnpar.v:39winered_bnn1_bnnpar.v:91winered_bnn1_bnnpar.v
T1388	IFO	Unsigned	5	I2 + I4 (winered_bnn1_bnnpar.v:43winered_bnn1_bnnpar.v:47winered_bnn1_bnnpar.v
T1690	IFO	Unsigned	6	I3 + T1388 (winered_bnn1_bnnpar.v:64winered_bnn1_bnnpar.v:83winered_bnn1_bnn
T1932	IFO	Unsigned	7	T1540 + T1690 (winered_bnn1_bnnpar.v:179winered_bnn1_bnnpar.v:183)
T1928	IFO	Unsigned	8	T1548 + T1932 (winered_bnn1_bnnpar.v:183)
T1954	IFO	Unsigned	6	I1 + T1994 (winered_bnn1_bnnpar.v:63winered_bnn1_bnnpar.v:184)
T1333	IFO	Unsigned	6	I8 + T1388 (winered_bnn1_bnnpar.v:43)
T1609	IFO	Unsigned	7	I11 + T1548 (winered_bnn1_bnnpar.v:40winered_bnn1_bnnpar.v:44winered_bnn1_bn
T98	IFO	Unsigned	5	I1 + I3 (winered_bnn1_bnnpar.v:44winered_bnn1_bnnpar.v:52winered_bnn1_bnnpar.v
T1950	IFO	Unsigned	6	T98 + T1540 (winered_bnn1_bnnpar.v:44winered_bnn1_bnnpar.v:135)
T1948	IFO	Unsigned	8	T1609 + T1950 (winered_bnn1_bnnpar.v:44)
T1946	IFO	Unsigned	8	I8 + T1950 (winered_bnn1_bnnpar.v:135)
T1595	IFO	Unsigned	8	T1388 + T1609 (winered_bnn1_bnnpar.v:136)
T1944	IFO	Unsigned	6	T1388 + T1540 (winered_bnn1_bnnpar.v:68winered_bnn1_bnnpar.v:75)
T2040	IFO	Unsigned	8	T1944 + T2045 (winered_bnn1_bnnpar.v:75)
T1714	IFO	Unsigned	7	I8 + T1548 (winered_bnn1_bnnpar.v:67winered_bnn1_bnnpar.v:107winered_bnn1_bn
T1704	IFO	Unsigned	8	T98 + T1714 (winered_bnn1_bnnpar.v:67)
T1940	IFO	Unsigned	8	I11 + T1944 (winered_bnn1_bnnpar.v:68)
T1875	IFO	Unsigned	5	I4 + I10 (winered_bnn1_bnnpar.v:94winered_bnn1_bnnpar.v:103winered_bnn1_bnn

Figure 10: An example of a datapath block's extraction report. An intermediate value that is reused multiple times is highlighted.

2.5.2 Implementation

A formulation of the problem is the following: Given a list of expressions of the general form $y_i = x_0 + x_1 - x_2 - ... + x_n$ in which operants can be shared between the expressions find the minimum number of additions or subtractions that need to be performed to evaluate all expressions.

The problem turns out considerable less well-studied than initially expected. While the deceptively simple description suggests a straightforward way to answer it, it is NP-Complete difficult, more specifically in the MaxSNP family of optimization problems. As a direct result only approximate solutions are attempted. [guy] searches for exact solutions by leveraging SAT solvers, but only manages to get this to work for very small matrix sizes up to 8 x 8. Not much is else found on the exact scenario above, but a close-enough problem having to do with factoring similar lists of expressions of the form $y_i = x_0 \oplus x_1 \oplus ... \oplus x_n$ using the minimum possible XOR operations is actively worked on thanks to some applications in the field of cryptographic accelerators. Both belong to the shortest linear program family of problems.

I choose to try utilising Paar's factoring algorithm [paar] first. It is older than most heuristics that have been applied to the XOR factoring problem, but has the advantage of not exploiting term cancellation. Thanks to the property $x \oplus x = 0$ some optimal solutions to the XOR problem include two subexpressions containing the same term x being combined by XOR to produce a desired expression that does not include x. Heuristics developed after Paar's take advantage of this feature, and while there is a parallel between it and the term cancellation of opposites in our scenario ($x - x = 0$ or $x + -x = 0$) I have not managed to find the adjustments needed to apply their insights to the new domain. Thus I give precedence to the more straightforward method, that directly translates to using addition in place of parity.

2.5.3 Paar's algorithm

It is essentially a greedy algorithm that picks the two elements that are common in the largest number of expressions each time and adds the result of their XOR to the list of elements.

Let N be the number of inputs, M be the count of expressions to evaluate, x_i be the i-th input, y_i the i-th expression and $A \in M \times N$ be the binary matrix we aim to factor. The value of $A_{i,j}$ is set to 1 if the term x_j is included in the XOR expression y_i and 0 otherwise.

For example if $N = 4$ the expression $y_i = x_0 \oplus x_2$ corresponds to the row $A_i = [1010]$.

The following steps are repeatedly applied:

1. Find the two columns $A_{:,i}$ and $A_{:,j}$ that have the bitwise AND with the largest weight. This corresponds to the columns with the largest dot product, so they can quickly be calculated by $i, j = \arg\max_{k>l}(A^T A)_{k,l}$. This corresponds to finding the operation between two inputs or intermediate results that occurs the most times across all expressions.

2. Append the resulting product column $A_{:,N} = A_{:,i} \wedge A_{:,j}$ to A. Increase N by one to reflect the new width of the matrix. Intuitively this translates to including $x_i \oplus x_j$ as a new intermediate result x_N to be used in farther operations.

3. Set $A'_{:,i} = A_{:,i} \wedge \neg A_{:,j}$ and $A'_{:,j} = A_{:,j} \wedge \neg A_{:,i}$. Thusly the dependence of expressions to x_i and x_j is removed when it is now covered by the inclusion of $x_i \oplus x_j$ in them.

In the end only one element in each row has value 1, and the index j of the column the only 1 of the i-th row occurs in tells as the input or intermediate result the i-th expression equals, $y_i = x_j$.

Paar's algorithm can work for a group of expressions that consist only of addition, but the expressions we have to work with include both additions and subtractions. To reconcile this issue the negative of each input element is treated as a separate input element that is added where the original would be subtracted. Given the original weight matrix W with $W_{i,j} \in -1, 1$ denoting whether element x_j is added or subtracted from the expression y_i, we construct the matrix A we pass as the initial state to the algorithm by first turning all the -1 elements to 0 and then appending the inverse of the matrix to itself, or $A = \max(0, [W, -W])$.

From this process a list L of successive indices such that $L_n = (i, j) \iff x_n = x_i + x_j$ is acquired, and the additions implied by them are hardcoded in the verilog description of the designs.

2.5.4 Extension to support subtractions

I try a slight modification to the original procedure so it can be compatible with expressions including subtractions. The way I described previously to use negative inputs with Paar's strategy often has to unnecessarily repeat calculations. For a minimal example, the expressions $y_0 = x_0 - x_1 + x_2, y_1 = x_0 + x_1 - x_2$ would result in 4 operations ($x_3 = x_0 + -x_1, y_0 = x_3 + x_2, x_4 = x_0 + x_1, y_1 = x_4 + -x_2$), instead of the 3 needed ($x_3 = x_1 - x_2, y_0 = x_0 + x_3, y_1 = x_0 - x_3$). This can be avoided by taking the ability to subtract instead of only add intermediate results into account.

In summary this works by using {-1, 0, 1} for the elements of the matrix A, where $A_{i,j} = -1$ when the expression for y_i contains the negative of the value x_j. Instead of counting the number of $(1,1)$ pairs of elements for columns as before, the count of pairs of elements that are either $(1,1)$ or $(-1,-1)$ corresponds to the number of times the sum of the values is used, and the count of pairs of elements that are either $(1,-1)$ or $(-1,1)$ corresponds to the number of times the difference of the values is used. As before the operation that occurs in the most expressions is chosen as the next operation to be implemented.

Finding these two counts for all pairs of columns can still be done with a matrix multiplication like before so the new approach is not much slower.

2.5.5 Results and analysis

Table 4: Effect of preemptive arithmetic optimization with Paar's heuristic

	bnnparsign area(cm²)	bnnpaar area(cm²)	area change	bnnparsign power(mW)	bnnpaar power(mW)	power change
Har	24.52	17.42	-29.0%	78.8	57.2	-27.4%
cardio	33.27	38.74	+16.4%	106.2	124.1	+16.9%
gasId	175.09	281.55	+60.8%	499.1	807.6	+61.8%
pendigits	33.38	35.43	+6.1%	108.9	114.6	+5.2%
winered	22.45	18.55	-17.4%	74.6	62.6	-16.1%
winewhite	20.47	18.01	-12.0%	68	59.8	-12.1%

25

Table 5: Comparison of the modified Paar heuristic to the original

	bnnpaar area(cm²)	bnnpaarter area(cm²)	area change	bnnpaar power(mW)	bnnpaarter power(mW)	power change
Har	17.42	18.73	+7.5%	57.2	60.8	+6.3%
cardio	38.74	35.97	-7.2%	124.1	116	-6.5%
gasId	281.55	261.38	-7.2%	807.6	759.7	-5.9%
pendigits	35.43	32.22	-9.1%	114.6	107.3	-6.4%
winered	18.55	17.47	-5.8%	62.6	59.6	-4.8%
winewhite	18.01	16.65	-7.6%	59.8	55.9	-6.5%
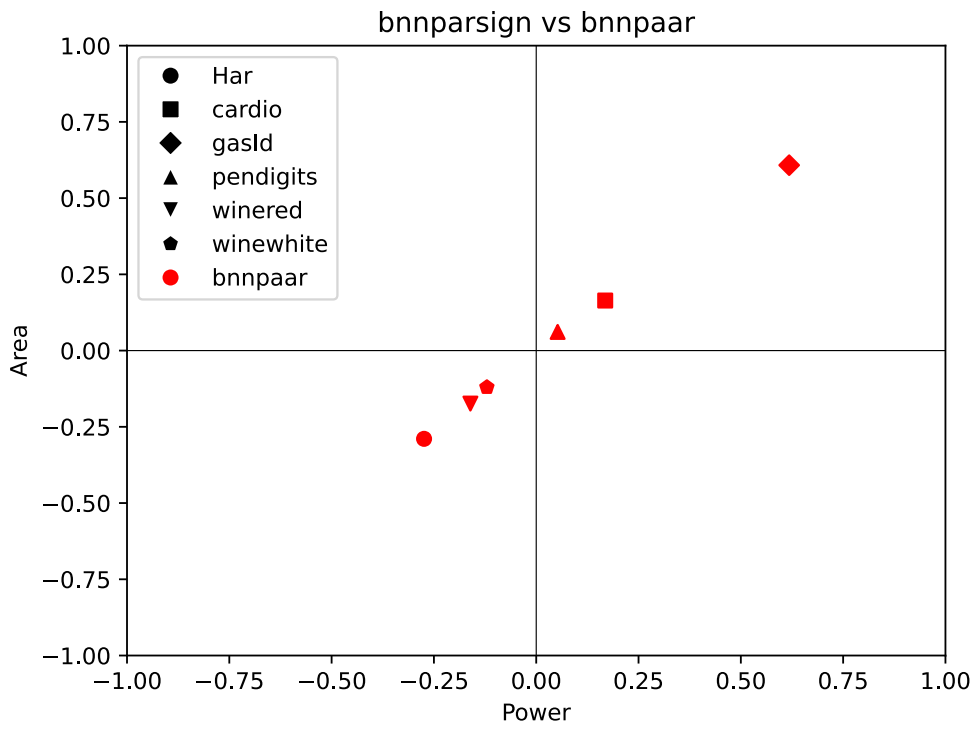
Figure 11: Effect of preemptive arithmetic optimization with Paar's heuristic
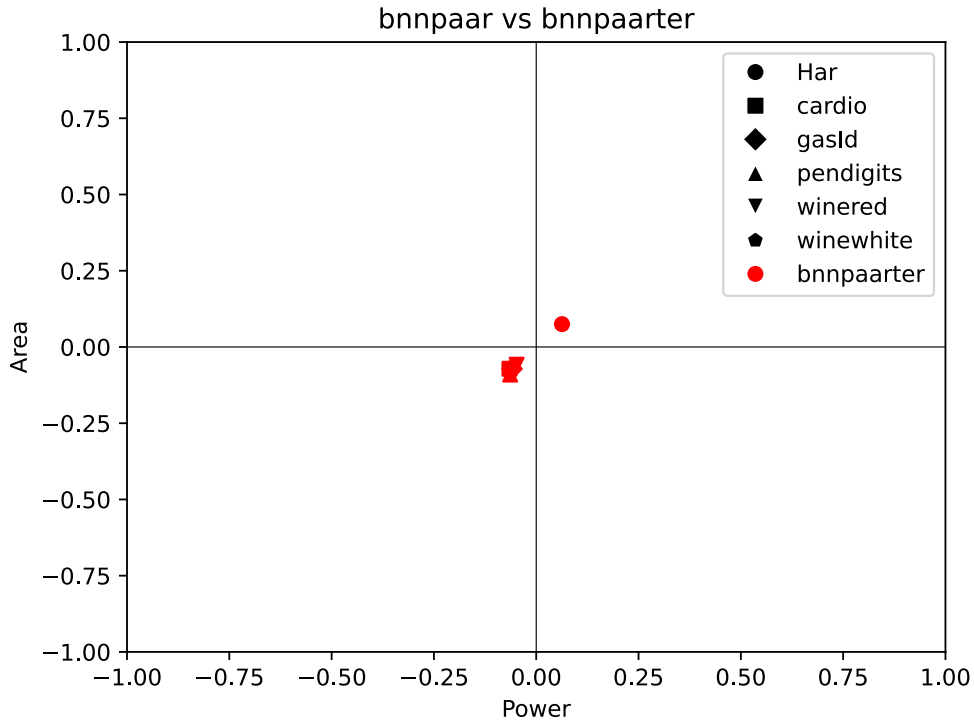
Figure 12: Comparison of the modified Paar heuristic to the original

I expected that either:

1. The results of hardwiring the order of operations for calculating the pre-activation result of the neurons using Paar's heuristic would be considerably worse than the result of letting Design Compiler use the results of it's own optimization heuristics, since they ought to have implemented the best known ones. In this case trying an alternative to preemptively optimise the operations beforehand is most likely wasted effort because finding a competitive heuristic would be harder than parsing the results of their solution.

2. The results would have a negligible difference, because the heuristics used are related and / or the quality of results that can be expected by current methods for reasonable compute budgets hits a certain ceiling for the various approaches. In this case applying approximation techniques to the estimated arithmetic operation graph can go ahead.

The results show that although it is not consistant across the networks, there is an improvement of 20-30% to the area and power estimates of the smallest ones. This causes suspicion, since if such an old and common algorithm performed better for some cases of the problem they would reasonably have simply used it already. I initially look for ways the original designs could be obstructing datapath extraction more than they should, but nothing jumps out to me.

There seems to be a scaling in effect where the size of the weight matrix or the number of total operations are inversely correlated with how well Paar's algorithm performs compared to the compiler's unknown solution. I hypothesise that they chose the methods they did for arithmetic optimization giving more weight to the performance on heavier workloads, where the savings are more important, or alternatively the trade-offs these methods consider apply better to heavier loads. This leaves some wiggle room for improvement in the sizes of the examined networks.

Unfortunately, the issue I am trying to address has to do with performance losses from disrupting compiler's arithmetic optimizations scaling with model size, and the relative performance of the alternative heuristic scales inversely with that size. This means that the attempted fix cannot apply to the cases that need it most, so the underlying problem remains unresolved.

The ternary take on Paar's heuristic outperforms the original by a relatively consistant ratio with exception of the Har model's network. This gives me some hope that applying more advanced heuristics used in Shortest Linear Programs modefied for this particular usecase would raise the network size threshold for which results can be improved.

3 Sequential Evaluation of Layer Neurons

3.1 Single Input, Per-Cycle Update

3.1.1 Rationale

The classifications considered here are mostly not time critical and do not require high throughput. Evaluating the quality of a wine every second or multiple times per second does not offer any more value than doing it every few minutes. Since time is the less precious resource for our purposes it can be traded for lowering area and power demands.

A way to approach this trade-off is by extending evaluation of neurons' values to multiple clock cycles so that the adder graphs needed to perform all of the numerical operations can be replaced with simpler adder circuits that get reused between cycles. This requires the inclusion of memory elements to hold intermediate results of calculations between cycles.

I first try to make all neurons sequentially evaluate their pre-activation values by updating their held value on new inputs on successive clock cycles until they have included all of their input values into their total. This means that each layer will take as many cycles to calculate it's outputs as the number of input features it has. Layers get evaluated successively, so the entire inference will take a cycle count equal to the sum of all the inputs and hidden features of the network.
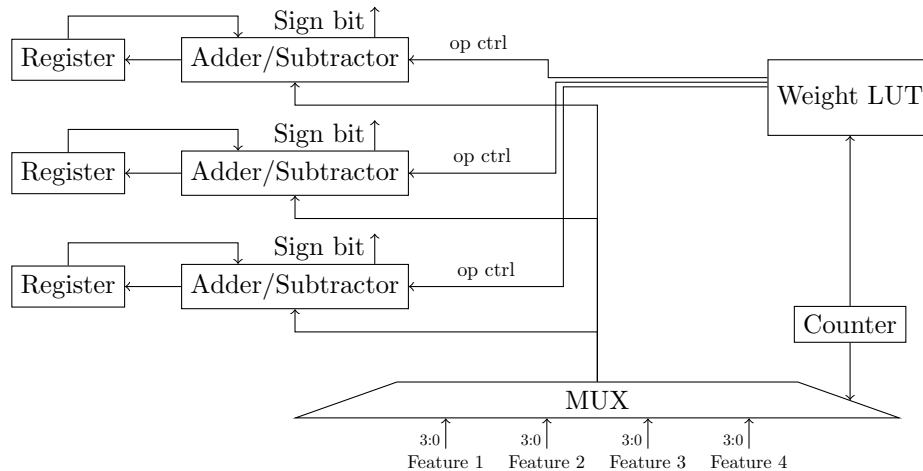
3.1.2 Implementation

Figure 13: The first layer of a sequentially evaluated BNN

29

3.1.2.1 First layer In the first layer each neuron is implemented by an accumulator that holds a running total of the weighted sum of the input features seem thus far and an adder-subtractor that given the weight bit of the connection between the neuron and the input feature currently updated on as a control either adds of subtracts the newly presented feature with the previous value of the accumulator to get next value of the accumulator. In each cycle a new input element is selected for all neurons of the layer and they either add it or subtract it from their running totals.

The weights of the layer are stored in a memory. A counter is used to select the current feature from a multiplexer and the column of the weight matrix from the weight memory that will provide the control signals to the adder-subtractors. When the value of the counter reaches the final value that indexes an input feature, $N-1$, a flag is set that stops the counter and the accumulators of the current layer from updating their held values and signals the next layer to start it's own process. A reset signal is used to bring these memory elements back to their zeroed initial values when inference of the next set of inputs is desired. A reset is required to happen before each inference starts.

Let k be the number of cycles since the start of the inference / the current value of the counter. $h_{i,k}$ be the value of the accumulator of the i-th neuron on the k-th cycle, or after updating on the first k input elements. Clearly $h_{i,0} = 0$ and $h_{i,N-1}$ would be equal to h_i. x_k is the input element selected on the k-th cycle and $h'_{i,k}$ is the output of the adder-subtractor of the i-th neuron at the end of the k-th cycle.

$$h_{i,k+1} = h'_{i,k} = h_{i,k} + x_k = \sum_{j=0}^{k} x_j$$

Because the output of the add-subtract unit when the last input of the layer is selected is equal to the pre-activation value of the neuron, this value does not have to be stored in the accumulator to be used. Instead the sign bit that determines the binarized output of the neuron for the next layer can be taken directly from the adder-subtractor's output. This way the first layer can be evaluated in $N-1$ cycles instead of N, as long as the selected input of the first layer stays at the last ($N-1$-th) position for the duration of the second layer's evaluation.

An alternative implementation where the weight matrix was stored in shifting registers instead of a constant array indexed by the counter was tested. The memory elements are very expensive in this technology so this version ended up underperforming the previous by a large margin due to the required registers.

3.1.2.2 Second layer The second layer starts after receiving an enable signal from the first layers halting flag. Because of the linear transformation described in the start in this layer instead of subtracting one from the running total when the weighted current input would be -1 instead 0 is added to the running total, so it remains unchanged. It could be implemented similar to how the first layer is implemented if the adder-subtractors are exchanged with XNOR gates, by storing the weights of the layer in a memory and calculating the XNOR of the weight column $W2_{:,k}$ with the output bit of the previous layer s_k to add to the running totals on the $k+1$-th cycle.

Instead , each neuron gets it's own multiplexer over input features, where the k-th data line of the i-th neuron's multiplexer is set to be s_k if the weight $W2_{i,k}$ of the connection between the hidden feature s_k and the neuron y_i is 1, and $\neg s_k$ in the case it is -1. This is equivalent to hardcoding the result of the XNOR operation for that particular neuron as the data line of the multiplexer.

In each cycle the neuron receives a single bit and adds it to the value in its accumulator. It can therefore be implemented via a counter with this bit as an enable signal.

The main goal of this approach is to remove the need for storing theweights of the layer and the decoder to select them, not the negligible XNOR gates that would be used. These multiplexers share their input data lines with a lot of the other multiplexers, so the hardware cost of their implementation is considerably cheaper than C separate ones.

3.1.3 Results and analysis

Table 6: The first attempt at a sequential implementation compared to the combinatorial one

	bnnparw area(cm²)	bnnseq area(cm²)	area change	bnnparw power(mW)	bnnseq power(mW)	power change
Har	24.25	29.55	+21.9%	77.6	132.7	+71.0%
cardio	33.21	31.47	-5.2%	105.4	143.1	+35.8%
gasId	171.37	47.67	-72.2%	486.9	216.8	-55.5%
pendigits	33.97	34.71	+2.2%	109.6	139	+26.8%
winered	21.87	29.57	+35.2%	72.3	131.7	+82.2%
winewhite	20.36	29.75	+46.1%	66.7	128.6	+92.8%
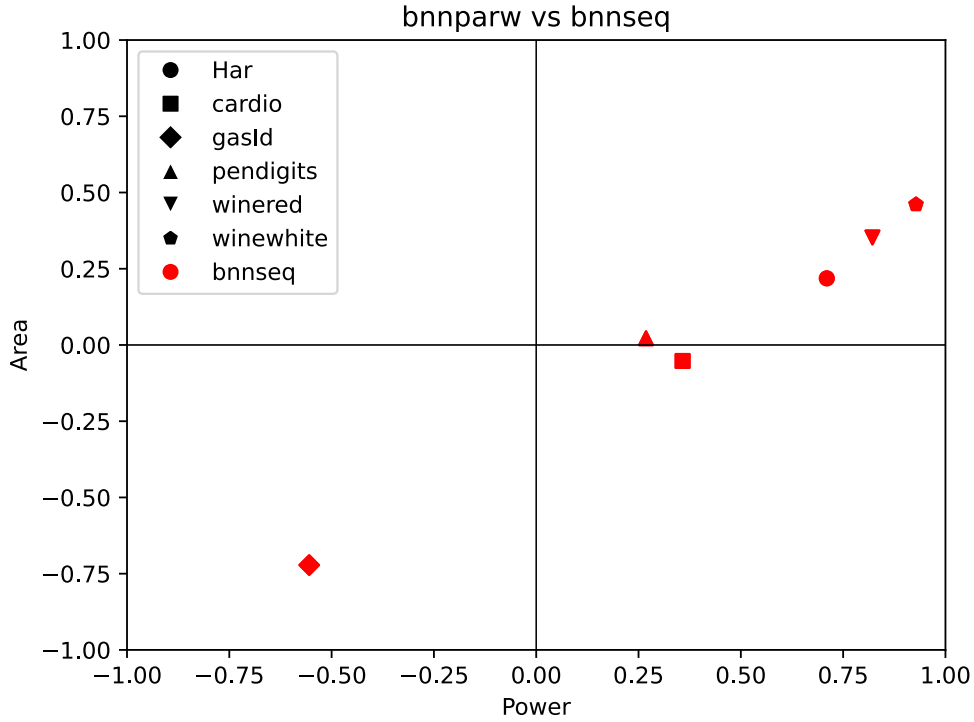
Figure 14: The first attempt at a sequential implementation compared to the combinatorial one

The cost of the adder graph in the fully parallel designs scales superlinearly with the count of input elements of the layer, at a faster rate than multiplexers and decoders used in these sequential designs, and the number of required registers scales about logarithmically. It is expected then, that the advantage of a sequential to a parallel design would also scale to the number of input features N.

The expense of the sequential elements is also pronounced in this technology, and since as mentioned before it doesn't increase by much due to additional inputs, a clear disadvantage is given to the smaller networks, exaggerating the scaling effect.

Most of the networks under examination are small enough to be in the range that is disadvantaged by the change, with the smallest ending up 50% larger. Only the largest model's network, with 128 input features, is clearly gaining anything from this trade-off, as the sequential design takes up 70% less area.

Perhaps the upfront cost can be lessened, which would be bring littler networks into the range that benefits from this sequential design area wise. Even if the way to achieve this ends up diminishing the scaling benefits described above, it can be applied only to models with N lower than a threshold, so it would not be an issue.

3.2 Removing the weight array
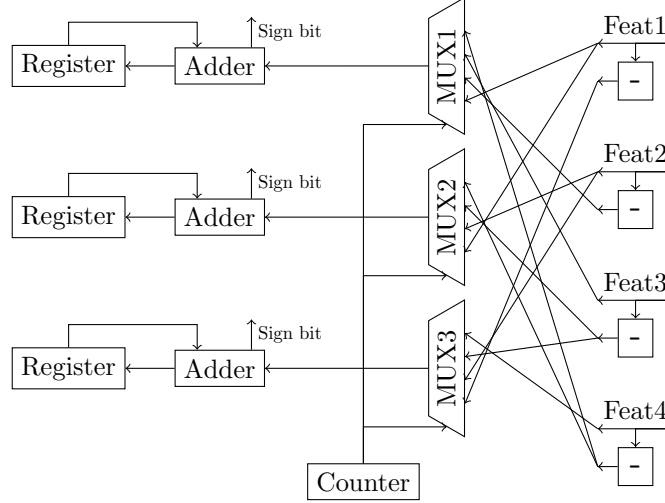
Figure 15: The first layer of a sequential design with the required subtractions hard-coded

The process used in the second layer in the previous part, where each neuron gets its own multiplexer over normal and inverted input hidden features in order to have no need of a weight memory, is here applied to the inputs of the first layer as well.

For a hidden neuron h_i the j-th data line in its multiplexer will be denoted $x_{i,j}$. The data lines of the multiplexer will be 5 bit signed integers, so they can represent the values of the 4 bit input features as well as their negatives. Similarly to how a data line in the second layer described above would be set to either s_k or $\neg s_k$, the data lines in the first layer are set as such:

$$x_{i,j} = \begin{cases} x_j, & \text{if } W1_{i,j} = 1 \\ -x_j, & \text{if } W1_{i,j} = -1 \end{cases}$$

The adder-subtractors and the weight array with the decoders that selected the control signals from them are removed. Since the input is taken already negated when appropriate, only an adder is needed for the accumulator.

Although some up-front costs are gone, the extra machinery to negate each input feature and for the custom multiplexers makes each input more expensive. The largest network, gasId, is as such almost doubled in required area, but this change

34

was aimed for the smaller networks. It manages up to 8% improvement there, which is nowhere near enough to break even with the parallel version.

3.3 Register width reduction

The number of bits the register of the accumulator of each neuron can be reduced to the minimum required to support the range of values it encounter in the dataset. This is exactly the same bitwidth reduction as the one described for the parallel design. Each bit shaved off an accumulator's range removes a flip-flop.

Because the registers take up a significant chunk of the resources, the improvement is more pronounced than in the fully parallel equivalent, freeing up around 10% of the area and power across the board.

3.4 Accumulator saturation
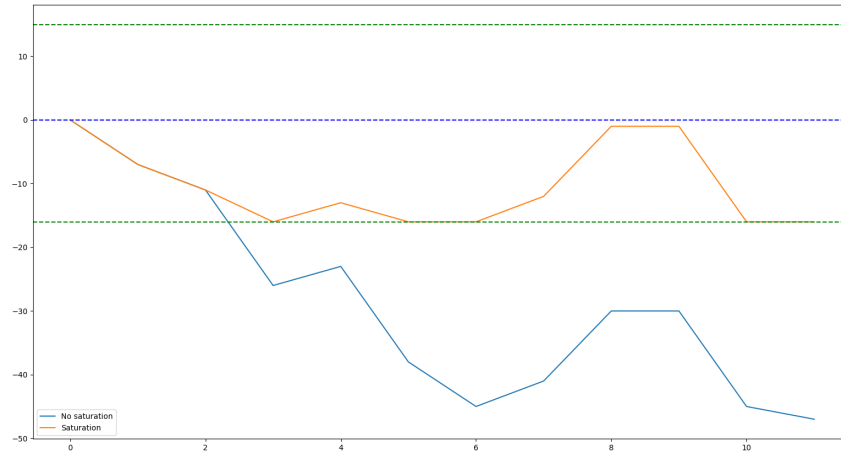
Figure 16: Value of a neuron's accumulator over the course of the evaluation, with and without saturation of the results

Since removing flip-flops by reducing the bitwidth of the registers appears to help alleviate the up-front cost of changing to sequential evaluation for smaller networks, expending some extra combinatorial logic to lead to further shortening can be justified. The method to do that approached here is by saturating the results of the addition between the previous running total stored in the register and the new input feature to stay in the bounds of a smaller range.

The result h_i that is found for the neuron i at the end of the layer's evaluation does

not need to be the actual weighted sum of the input features it is supposed to represent. Since binarization of the result occurs before it is passed to the next layer, an approximate result does not lead to an error in the neuron's output s_i as long as it still has the same sign as the original.

If at some cycle during the layer's evaluation the absolute value of the running total becomes sufficiently large, it becomes unlikely that the remaining features will add up to be even larger in the opposite direction without overshooting the difference by some distance. This means we can saturate the intermediate results to a range $[-2^r, 2^r - 1]$ without much risk the final aggregate having the wrong sign.

Take the case where k is the last cycle the value of the accumulator gets saturated to -2^r. In order for an error in the output to occur because the sign of the accumulated value in the end flips to positive when it would not if the full range of values was supported, the weighted sum of the remaining features that will be added in the next cycles must be larger than 2^r, but smaller than the true running total.

$$2^r \leq \sum_{j=k}^{N-1} \leq \sum_{j=0}^{k-1}$$

The smallest value of r is found for each neuron such as this case or its equivalent in the opposite direction do not occur for any samples in the dataset. The bitwidth of the accumulator of that neuron is then set to $r + 1$ and the results of the addition of a feature are saturated to that range using the DW_addsub_dx module from designware, if and only if $r + 1$ is smaller than the width the neuron was previously reduced to that fit it's entire range of values. In the case that width is the same as $r + 1$, saturating the values is not allowing the flip-flops of the accumulator to decrease and there is no benefit to incur the extra logic of implementing saturation for this neuron.

Figure 17: Implementation of saturation on the first layer of a sequential design.

3.5 Results and analysis

Table 7: Effect of the mentioned improvements to the sequential design

	bnnseq area(cm²)	bnndsat area(cm²)	area change	bnnseq power(mW)	bnndsat power(mW)	power change
Har	29.55	24.02	-18.7%	132.7	109.2	-17.7%
cardio	31.47	24.77	-21.3%	143.1	118.7	-17.1%
gasId	47.67	81.05	+70.0%	216.8	318.9	+47.1%
pendigits	34.71	29.79	-14.2%	139	121.6	-12.5%
winered	29.57	23.02	-22.2%	131.7	104.5	-20.7%
winewhite	29.75	22.43	-24.6%	128.6	98.5	-23.4%

Figure 18: Effect of the mentioned improvements to the sequential design

After these improvements, 4 out of the 6 networks demand less area in the sequential design than in the parallel one. But the impovement is not substancial enough to justify evaluation taking up many more cycles, and the power is still not competitive with the parallel designs. This tells me that this version of sequential designs is not salvageable. A different process of splitting the workload among cycles must be constructed from the ground up.

3.6 Single adder tree sequential evaluation

3.6.1 Rationale

Since the previous attempt where all neurons update in parallel on a single input feature each cycle did not pan out, the clear next candidate is an arrangement where a single neuron of the layer updates on all input features in parallel in a given clock cycle. This means that a single adder tree will calculate the total value of a neuron h_i by summing up the weighted features in a single cycle, and perform the same for a different neuron of the same layer in the next cycle.

This way the adder graph that encompasses the calculations required for the entire layer in the fully parallel version gets reduced to the adder tree a single neuron's inference demands. This can more than make up for the encoding of weighting the features appropriately before their accumulation than must now be done since the operations are not simply hard-coded into the circuit.

3.6.2 Implementation

Figure 19: A single-adder sequential BNN implementation

The multiplexing that was described in the previous sequential design is rearranged here in the sense that the M multiplexers with N data lines each turn into N multiplexers of M elements. Instead of a multiplexer belonging to a certain neuron and selecting the weighted feature that neuron should increment by this moment, now a multiplexer corresponds to a specific input feature and selects which "weighting"

of that feature the currently examined neuron needs. It is analogous to having the axis flipped.

Let's call the value selected to represent the j-th input feature on the i-th cycle of the layer's evaluation $x_{i,j}$. The way it is derived from the original input x_j is as stated before:

$$x_{i,j} = \begin{cases} x_j, & \text{if } W1_{i,j} = 1 \\ -x_j, & \text{if } W1_{i,j} = -1 \end{cases}$$

The functional difference is that the counter is indexing on the value i instead of j. Like before the negation only happens once per input.

The selected weighted inputs are then parsed by a generic N input adder tree that provides the sign of their sum, on the i-th cycle $s_i = sign(\sum_{j=0}^{N-1} x_{i,j})$. Only the sign bit needs to be stored to be available to following calculations by the next layer, the pre-activation value h_i can be safely discarded. A 1-bit register is thus indexed by the counter to store the current neuron's output. This process takes as many cycles to evaluate a layer as count of its neurons, so M clock cycles for the first layer.

A close to identical system as the previous approach detects when the last neuron of the layer has finished operations and passes the torch to the next layer to start. The next layer conditionally inverts the input features it receives before passing them to multiplexers' data lines on the logic the first layer negates them.

On the second and final layer results do not need to be stored at all. Because the output of neurons is calculated one at a time, the argmax operation can be embedded in this process. Two registers are used, one holding the largest output of a neuron seen so far y_{max} and the other the index of the aforementioned neuron in the layer, which is taken from the value of the cycle counter of the layer.

If the result of the popcount operation on the current weighted inputs on the i-th cycle of the second layer's activity y_i is greater than the previous best y_{max}, the new result is stored as the new best so far and the index is overwritten by the cycle count i. Beyond saving a lot of flip-flops the overhead of the additional argmax module that had to be activated after the second layer is removed.

The second layer takes as many cycles as classes to be examined for prediction. The full inference therefore takes up $M + C$ clock cycles. Again a reset signal must be given between successive inferences.

3.6.3 Results and analysis

Table 8: Comparison of single adder tree sequential designs with equivalent combinatorial designs.

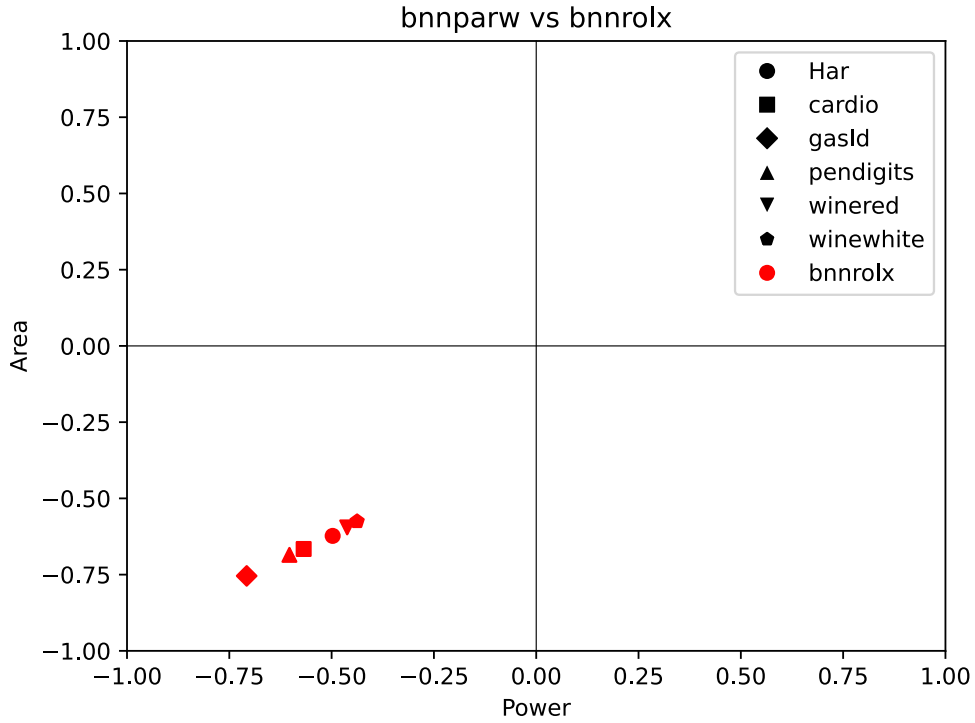|	bnnparw area(cm²)	bnnrolx area(cm²)	area change	bnnparw power(mW)	bnnrolx power(mW)	power change
Har	24.25	9.14	-62.3%	77.6	39	-49.7%
cardio	33.21	11.1	-66.6%	105.4	45.5	-56.8%
gasId	171.37	42.12	-75.4%	486.9	142.4	-70.8%
pendigits	33.97	10.69	-68.5%	109.6	43.5	-60.3%
winered	21.87	8.85	-59.5%	72.3	38.9	-46.2%
winewhite	20.36	8.65	-57.5%	66.7	37.5	-43.8%

Figure 20: Comparison of single adder tree sequential designs with equivalent combinatorial designs.

A large improvement on the previous sequential design method, using a single adder tree gets us 60 - 75% smaller footprints than the fully parallel circuits. Given the delay of the inference has been multiplied by a factor between one and two orders of magnitude this trade-off is kind of underwhelming. Like before an upfront cost in multiplexers / weight storage has to be paid upfront, and since the sizes of the networks are on the small side the scaling savings of reusing logic accross neurons do not deliver in full. The constraint reminds me of Amdaul's law, where instead of the speedup achievable by providing N parallel cores being limited by the ratio of the computation that is sequential, the resource savings are constrained by the ratio of hardware that can be shared between the N parallel cores.

Combinations of sequential approaches on the two layers where also tested to confirm that it was an improvement for both of them.
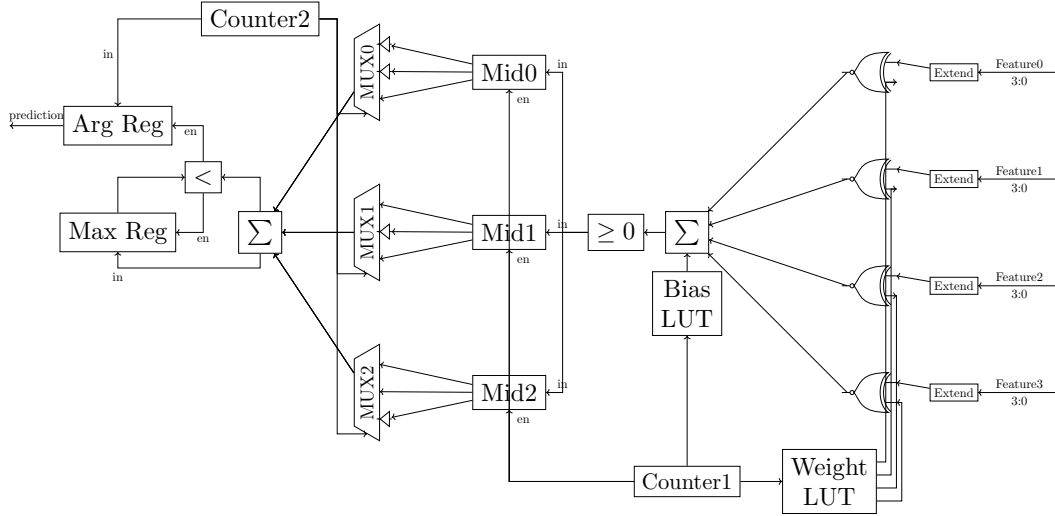
3.7 Deconstructing input negation

Figure 21: Multiplexers replaced by lookup tables for weights and correction terms/biases.

Negating each input involves a 4 bit increment-by-1 circuit per feature. Although it does not sound very alarming it is still an expense that scales with the input count N. The negation operation can be deconstructed into inverting the input and adding 1 to the result. If instead of providing the negative of the input as the result of multiplying by the appropriate weight to the multiplexer the inverse of all the bits of the input are provided, entire section simplifies into a 1-bit look up table indexed by the cycle counter whose output gets XOR'ed with all the bits of the input feature. This saves some logic.

In order to not risk errors from this approximation a correction term b_i needs to be added to the sum, equal to the number of 1s that were not added to negate in this cycle, or the count of elements of the weight row that belongs to the currently computed hidden neuron that are -1.

$$b_i = \sum_{j \in W1_i} [j = -1]$$

$$h_i = \sum_{j=0}^{N-1} x_j \oplus \neg bin(W1_{i,j}) + b_i$$
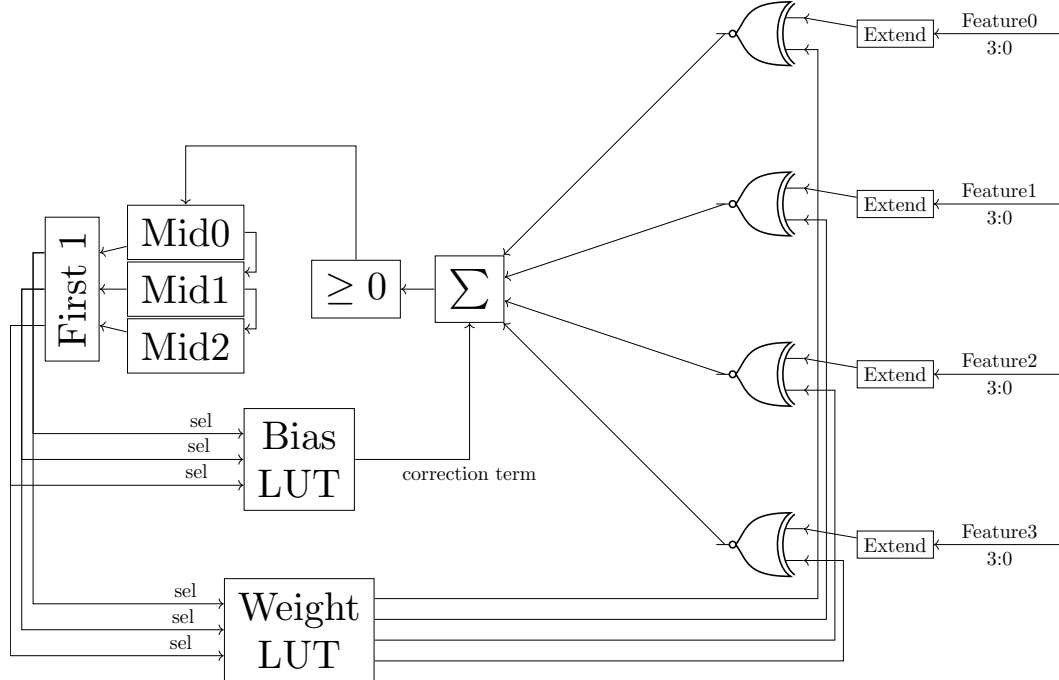
44

3.8 Shifting registers for timekeeping

Figure 22: Replacement of cycle counter by shifting registers for the hidden activations.

Instead of having a decoder from the cycle counter's current value i select the register to which the binary post-activation output s_i of the neuron that was computed will be saved, it is simpler to use a shifting register. Each cycle the previously held values are shifted one position to the right and the result of the current evaluation is saved to the left-most position of the register. After N cycles pass the right-most position of the register contains the result of the first neuron's evaluation that has been shifted $N - 1$ positions and all outputs are in their proper place. The flag that halts the operation of the first layer is then set and the results are frozen in place to be used by the next layer.

The inclusion of a shifting register where the values set on initialisation are discarded provides and opportunity to shed the cycle counter altogether. When the reset signal brings the registers to their pre-set values we assign the left-most bit to be 1 and all the rest to 0. The position of the most significant 1 in the register is shifted once to the right every cycle. By utilising a simple one-hot equivalent of a priority encoder

a M bit signal of a one hot representation of the current cycle count is produced.

This one hot signal can be used to detect when the final neuron is evaluated and layer transition flag ought to be set, and can select the weight row for the at the moment computed from the lookup table without requiring a decoder from the cycle counter. This lets the counter to be retired, without requiring extra state keeping elements to preserve its functionality.
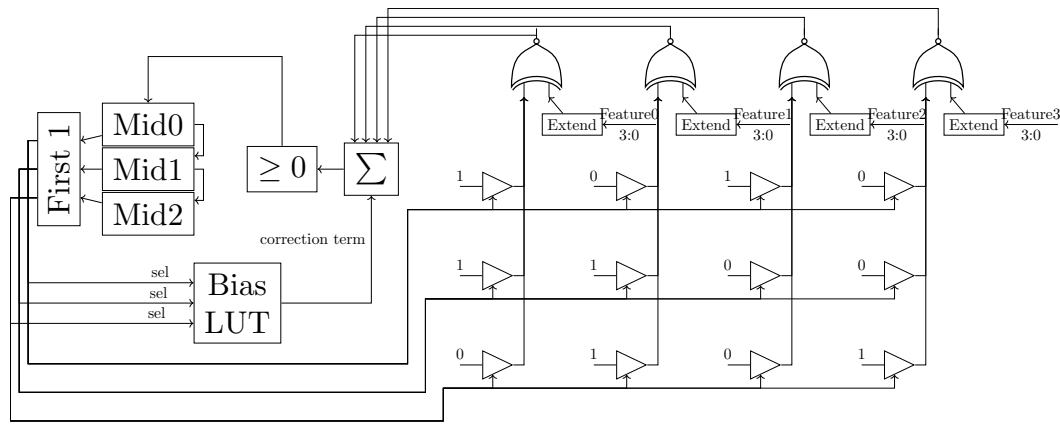
3.9 Tristate weight memory

Figure 23: Implementing the one-hot indexed weight memory using an open bus per input feature

Every input feature gets the current weight bit from an open bus to which a tristate buffer for each entry in the feature's column in the weight matrix is connected. Each buffer corresponds to a single element of the weight matrix $W1$. The tri-buffer that holds the value of $W1_{i,j}$ has its output connected to the same open bus as the other buffers that hold a weight in $W1_{:,j}$ and activates by the i-th bit of the one-hot select signal from above.

The goal of this is to avoid the nested OR gates that are used to reduce the selected value of the column into one bit in the standard look up table implementation.

3.10 Results and analysis

Table 9: Comparison of the final sequential designs to the final combinatorial designs

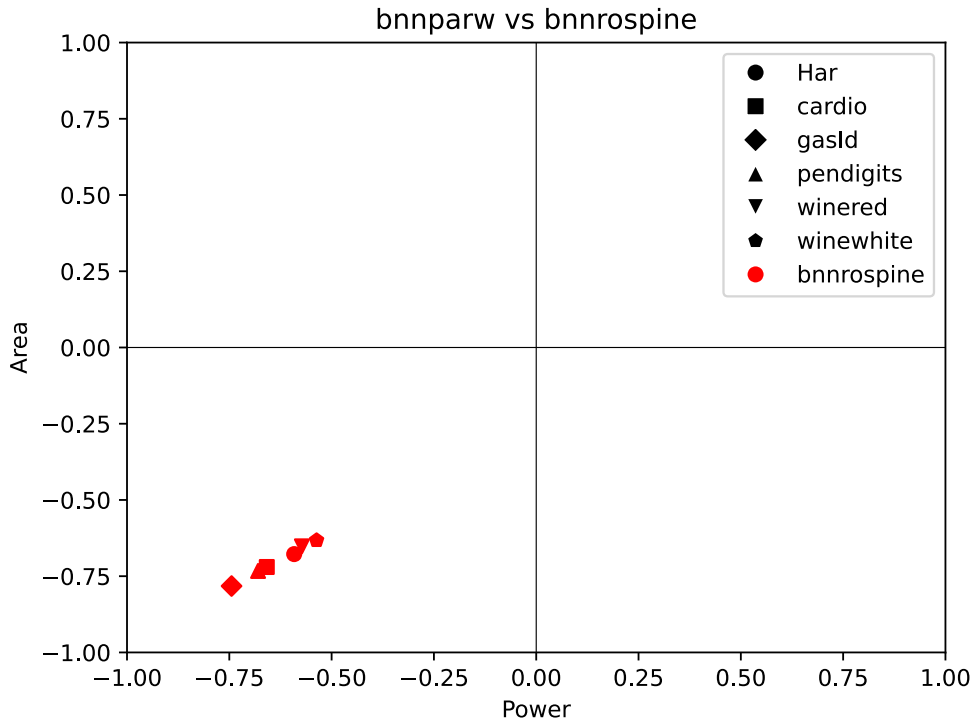|	bnnparw area(cm²)	bnnrospine area(cm²)	area change	bnnparw power(mW)	bnnrospine power(mW)	power change
Har	24.25	7.82	-67.8%	77.6	31.7	-59.1%
cardio	33.21	9.3	-72.0%	105.4	36	-65.8%
gasId	171.37	37.31	-78.2%	486.9	124.4	-74.5%
pendigits	33.97	9.08	-73.3%	109.6	35.1	-68.0%
winered	21.87	7.61	-65.2%	72.3	30.9	-57.3%
winewhite	20.36	7.49	-63.2%	66.7	30.9	-53.7%

Figure 24: Comparison of the final sequential designs to the final combinatorial designs

These changes give a 10-20% decrease in area and power requirements compared

to the initial single adder tree implementation. With the use of tristate buffers the power saving goes up to ~35% but at a very harsh area penalty of 10-30% compared to the first design. I think the explanation for this is that more tristate buffers are required than OR gates since logical simplifications cannot be made on them, but the considerable switching power consumption from the intermediate nets that connect nested OR gates is removed. This trade-off allows to optimise for whichever of area and power is the largest bottleneck to the desired application.

Importantly for our purposes, none of the models could be powered by a 30mW BlueSpark using a conventional LUT for the weights. After implementing the LUT using tristate buffers, 5 out of the 6 can be powered by it. Although not coming cheaply in terms of area, the power savings were critical for overcoming this barrier.

All in all compared to the fully parallel designs requirements are reduced $3 - 5\times$. This opens up the space of implementable applications. The relative savings would get considerably better for larger networks given the scaling observed.
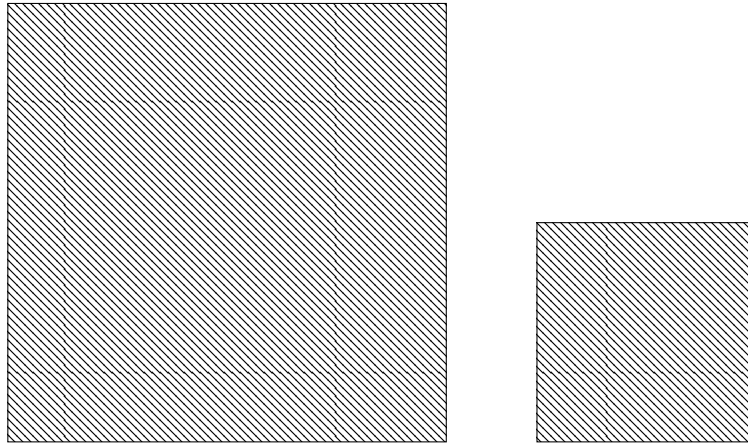

Figure 25: Actual size comparison of the estimated area of the printed designs for the pendigits dataset's model. Parallel on left, sequential on right.

4 Ternary weight networks

4.1 Rationale

Ternary Neural Networks (**TNNs**) use weights and activations in the range of {-1, 0, 1} instead of the {-1, 1} of BNNs. This enables much greater representational ability, and thus higher accuracies are achievable.When computed with CPUs or GPUs the inclusion of the 0 makes the bit-level operations that make BNNs so compute friendly not applicable, since the activations and weights now take up two bits and their MAC operations are not reducible to XNORs and popcounts. With hardware dedicated to running TNNs implemented in FPGAs or ASICs more optimizations can be made, but the efficiency is still sub-par compared to binary networks.

In our case the designs are fully bespoke to a single model/set of weights. This enables the isomorphism between ternary weight networks and sparse binary weight networks to be exploited, since connections removed from the sparse network can be omitted from the design upfront, something that is not doable in the case that all models of a certain architecture must be supported.

For the single-cycle / fully combinatorial designs this translates to fewer arithmetic operations to build components for. The model accuracy and the resulting circuit's area / power demands are both improved in this way by switching to ternary weights, pretty good deal.

Only the weights but not the activations will be ternarized in this implementation. The additional model ability achieved by using ternary activations for the hidden layer on top of the weights was not significant enough to justify the suspected cost of implementing 2-bit arithmetic in the subsequent layer.
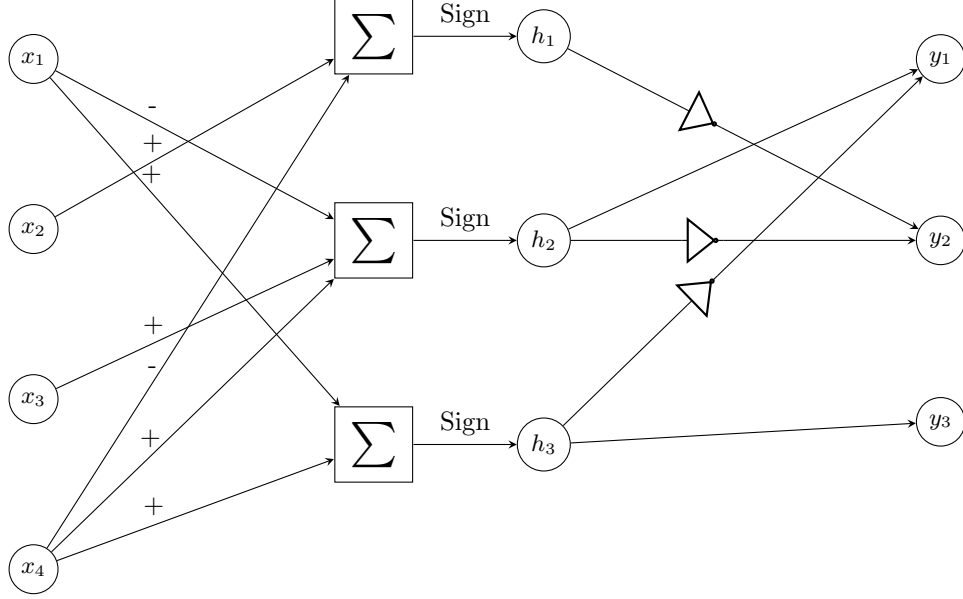
4.2 Fully combinatorial implementation

Figure 26: Sparce combinatorial single signed sum implementation.

After training the same datasets with the same parameter counts using ternary instead of binary weights the equivalent weight matrices $W1 \in \{-1, 0, 1\}^{M,N}$ and $W2 \in \{-1, 0, 1\}^{C,M}$ are used to define the desired operations similarly to the binary counterparts:

$$h_i = \sum_{j=0}^{N-1} \begin{cases} +x_j, & \text{if } W1_{i,j} > 0 \\ -x_j, & \text{if } W1_{i,j} < 0 \end{cases}$$

$$y_i = \sum_{j=0}^{M-1} \begin{cases} s_j, & \text{if } W2_{i,j} > 0 \\ \neg s_j, & \text{if } W2_{i,j} < 0 \end{cases}$$

In the first layer for connections that have weights of 0 neither addition nor subtraction is actualised for the feature in the neuron's specified expression. It is simply ignored since it always contributes 0 to the sum.

Some neurons turn out to have all their non-zero weights have the same sign, either all being 1 or all -1. In such a case since the input features are all positive the sign of the multiply-accumulate result for this neuron will always be the same.

So the outputs of these neurons are hardcoded into constants to avoid unnecessary overhead.

In the second layer, as well, connections with weights equal to zero get neither the hidden feature they connect to nor it's inverse included in the related output neuron's popcount. The required logic is thus reduced in both layers by each connection severed.

Remember the linear transformation used to go from sums weight-activation products of {-1,1} to popcounts of XNORs that now encode the values that would be -1 as 0. To achieve $-1 \rightarrow 0$ and $1 \rightarrow 1$ $f(x) = \frac{(x+1)}{2}$ is that linear transformation. When applied to an array $v \in \{-1, 1\}^M$ binary values the sum is:

$$\sum_{i=0}^{M-1} f(v_i) = \sum_{i=0}^{M-1} (v_i + 1)/2 = \frac{1}{2} \sum_{i=0}^{M-1} v_i + 1 = \frac{1}{2} \sum_{i=0}^{M-1} v_i + \frac{M}{2}$$

In the last layer, that in this case is the second one, so far the number of inputs of all output neurons was the same, thus the factor $\frac{M}{2}$ could be omitted when comparing outputs between the neurons and the XNOR/popcount results can be used directly for the argmax calculations.

Now, since the output neurons are treated as sparse binary ones, they no longer have the same input count and therefore the constant term $\frac{M}{2}$ is no longer the same for the whole layer. The issue can also be described as elements with value 0 included in the vector v contributing $f(0) = \frac{1}{2}$ each to the sum after the linear transfomation, which is not reflected by ignoring them completely as done here.

In order to fix this issue a correction term equal to $\frac{z_i}{2}$ ought to be added to the result the XNOR/popcount computation gives, where z_i denotes the number of elements in the weight row of the i-th output neuron $W2_i$. This term can be large compared to the value of the popcount when a neuron is sparse enough, so instead we can add $\frac{z_i - \min\limits_{j=0}^{M-1} z_j}{2}$ as a smaller correction term, so the neuron with the least severed connections gets nothing added to it's popcount and the rest get theirs based on how many extra zeroed weights they contain compared to it.

In the design this is done by shifthing the result of the popcount once to the left and adding the count of zeroes over the minimum as is to it, giving us $2y_i + (z_i - \min\limits_{j=0}^{M-1} z_j)$. The results of the neurons can now be compared correctly.

If we were dealing with a layer that was using XNOR and popcount that was not the

final one the correction term $\lceil \frac{z_i - \min\limits_{j=0}^{M-1} z_j}{2} \rceil$ would instead be used as the threshold for binarization of the neuron's output instead of 0.

4.3 Results and analysis

Table 10: Performance of the ternary weight combinatorial implementation compared to the binary combinatorial

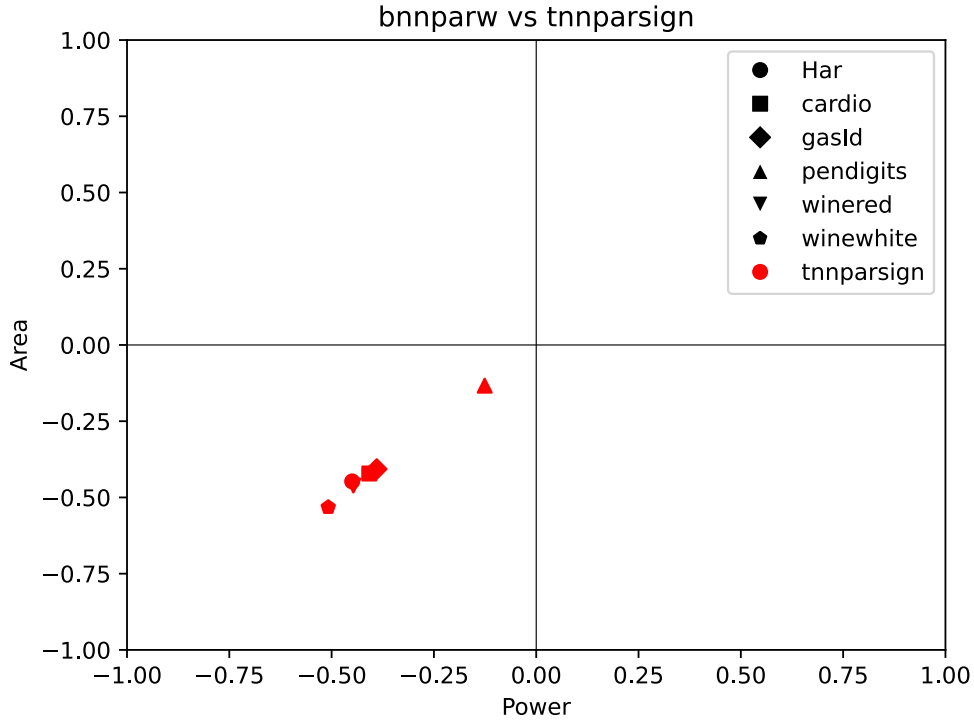|	bnnparw area(cm²)	tnnparsign area(cm²)	area change	bnnparw power(mW)	tnnparsign power(mW)	power change
Har	24.25	13.4	-44.7%	77.6	42.7	-45.0%
cardio	33.21	19.21	-42.2%	105.4	62.4	-40.8%
gasId	171.37	101.65	-40.7%	486.9	297.1	-39.0%
pendigits	33.97	29.43	-13.4%	109.6	95.8	-12.6%
winered	21.87	11.78	-46.1%	72.3	40	-44.7%
winewhite	20.36	9.53	-53.2%	66.7	32.8	-50.8%

Figure 27: Performance of the ternary weight combinatorial implementation compared to the binary combinatorial

Thanks to the removal of terms from the arithmetic operations that define the design of the layers the area and power requirements were almost halved compared to the fully combinatorial designs of the binary models that were trained on the same datasets as the ternary ones. The accuracy was also improved across the board while at it.

Unfortunately applying bitwidth reduction or pre-synthesis arithmetic optimization underperformed the original TNN circuits, even for datasets whose binary network implementations where improved by these methods. There is nothing to note on the implementation of these since no change needs to be made to accommodate TNNs. I am not sure what to make of this yet.

The attempts at sequential designs for ternary weight networks do not perform to a satisfactory level so they won't be expanded on.

5   Experimental setup

5.1   Data preparation

The files that comprise the 7 datasets described in the preliminaries where procured from the UCI repository. Afterwards using the descriptions of what each feature of the tabular dataset represents categorical features that could not correspond to a sensor's output are descarded. Additionally features that are constant or near constant (for example only 3 samples in the whole dataset have a different value for this feature from the rest) are removed since they could not provide useful information.

For each feature the range of values is then normalised in the $[0, 1]$ range so the features use similar scales. These values are then quantised in 4 bit precision by the formula $\lfloor x * (16 - \epsilon) \rfloor$, taking integer values in the range $[0, 15]$. This way the data is treated during training as if seen from a 4-bit ADC interpreting a sensor's analog output, like it is supposed to be under inference conditions.

The labels for each sample are enumerated so they take the range $[0, C - 1]$, which will later help with making the selection of the predicted class's index by the argmax module simpler. All of the datasets are finally converted into a standard format, that of a CSV file with one sample per row and feature per column and labels as the last column.

5.2   Training

The datasets are split randomly with a predetermined seed into a 70-30 split of training and test data.

All the training splits of the datasets are passed from a grid hyperparameter search using 5 fold cross validation provided by scikit learn to find the best performing configuration set. This selected hyperparameter configuration is then used to train the final model. Ten training runs are performed with the previous training split getting further divided into a smaller training split and a validation split. The model originating from the training run of the ten that achieves the highest validation accuracy is chosen as the result of the whole training process. The accuracy achieved by this model on the test split is reported as the accuracy of the learned classifier.

The actual model was initially implemented using the Larq framework for quantised models and afterwards switched to using the similar Qkeras framework after it was empirically found to achieve higher performing classifiers.

Interestingly the models that were trained under the Larq framework benefited from

the inclusion of a batch normalisation layer whereas models trained with the Qkeras framework had their performance hindered by it. I have not yet found a convincing explanation for this difference. I will note here that not using a batch normalisation layer after the hidden layer is what allows the threshold that the output of the first layer's neurons are compared to in order to produce their binarized output to be always zero. So this discrepancy was another point for the preference of Qkeras over Larq.

5.3   Parameter optimization and encoding

The models resulting from the above process are stored in a predetermined location that is accessible by the script that uses the weight matrices and architecture details obtained by the saved model plus as well as the original dataset in order to compute some derivative information, such as the minimum required bitwidth of neurons or the order of operations given by preemptive optimization. These auxiliary results are then passed to the script that encodes them as well as the raw weight matrices into a form that can be used as part of template verilog file.

This can take the form of writing out bespoke verilog instructions to implement the calculations necessary that are specific to the model. More commonly this information is formatted as parameters that can be imported into the verilog template and determine the actualised primitives and submodules that get instantiated and their connections via conditionals in generate blocks.

Both styles are equally able to describe the desired actualised design and either style can be used for any occasion the other can. In practice generating verilog instructions was found to be more convenient for the simpler fully parallel designs, and parameterised modules were more easy to work with for the rest of the cases.

5.4   Design instantiation and functional verification

The formatted custom functionality in either form described above is embedded into a template verilog module via the use of the icarus verilog tool as a verilog preprocessor. The result is a verilog module that describes a custom implementation of the specific model that was used as input. This is fully standalone and the stored model or derived parameters are not needed from this point forward.

After the custom module is instantiated it is used to simulate evaluation of 1000 samples from the dataset it is associated with. The reason that only 1000 samples are used instead of the full dataset is simply to speed up the process, since the requirements for exact execution are not so strict in our case that it is necessary to be

fearful of a potential error that does not materialise once in 1000 samples. Even if execution of the design does not precisely match the functionality of the original model in some edge cases as long as the classification accuracy is not measurably affected we are in the clear.

The results of the simulation are compared to those of evaluating the trained model in it's native framework for these same samples, and if everything matches up the process can continue. Note that a case where the design is found to not match the model's results is not expected to occur during hypothetical execution of the process by an actual user, the main goal of this simulation is for debugging purposes during development of the design template.

5.5   Synthesis and requirement evaluation

The custom design is synthesised using Design Compiler. The compilation is set to prioritise area efficiency and effectively no time constraint is given in order for timing optimizations not to interfere. The area estimation is taken from the compiler at this stage.

The netlist that was generated then goes under a gate-level simulation using Chrono-logic of the same 1000 dataset samples as the previous functional simulation to give realistic usage data for the estimation of the required power.

6 Results

Graphs and tables are presented here that show the area and power requirements for the various versions of hardware implementation for the 6 datasets and their trained models. Comparisons for the effect of the various design decisions outlined above that are not already displayed are also made.

The designs will be referred to by nicknames in the following graphs and tables. Here is which explanation of each design corresponds to each nickname:

Design nickname	Link to relevant description
bnnpar	Combinatorial fully connected implementations
bnnpar	Positive negative sum
bnnparsign	Signed sum
bnnparw	Minimum range bit width reduction
bnnparce	Range centering
bnnparstepw	Naively reducing bitwidths of intermediate results
bnnpaar	Preemptive arithmetic optimization
bnnpaarter	Extension to support subtractions
bnnseq	Sequential evaluation
bnndirect	Removing the weight array
bnndw	Register width reduction
bnndsat	Accumulator saturation
bnnrolx	Single adder tree sequential evaluation
bnnrolin	Deconstructing input negation
bnnrospine	Shifting registers for timekeeping
bnnrobus	Tristate weight memory
tnnparsign	Ternary weight networks

6.1 Dataset accuracies table graphs

6.2 Against cross-layer

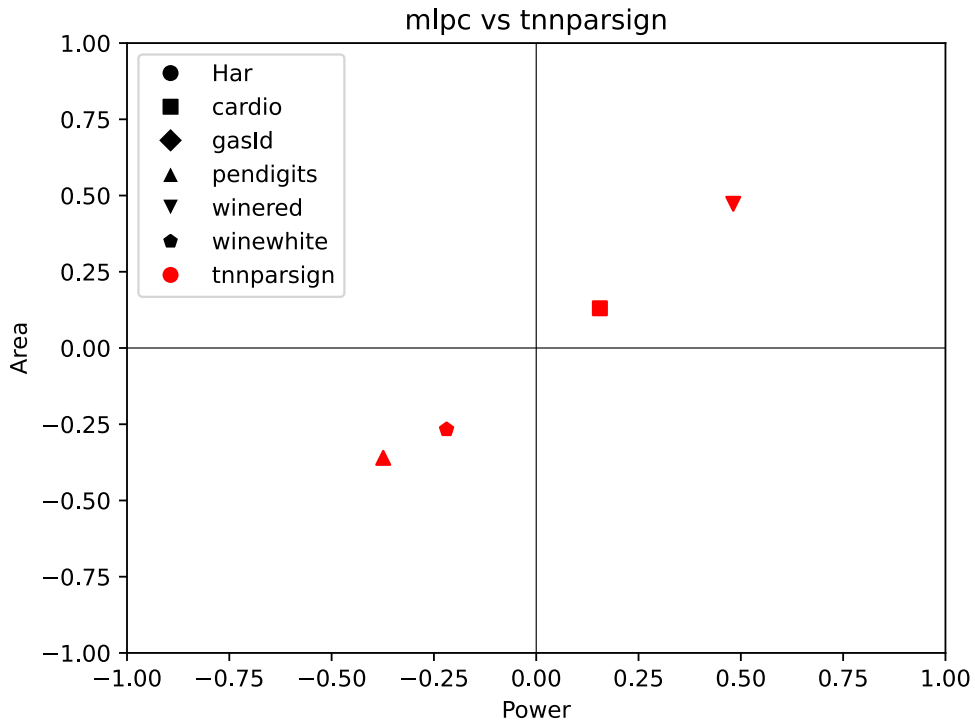|	mlpc area(cm²)	tnnparsign area(cm²)	area change	mlpc power(mW)	tnnparsign power(mW)	power change
cardio	17	19.21	+13.0%	54	62.4	+15.6%
pendigits	46	29.43	-36.0%	153	95.8	-37.4%
winered	8	11.78	+47.2%	27	40	+48.1%
winewhite	13	9.53	-26.7%	42	32.8	-21.9%

Figure 28: mlpc_tnnparsign

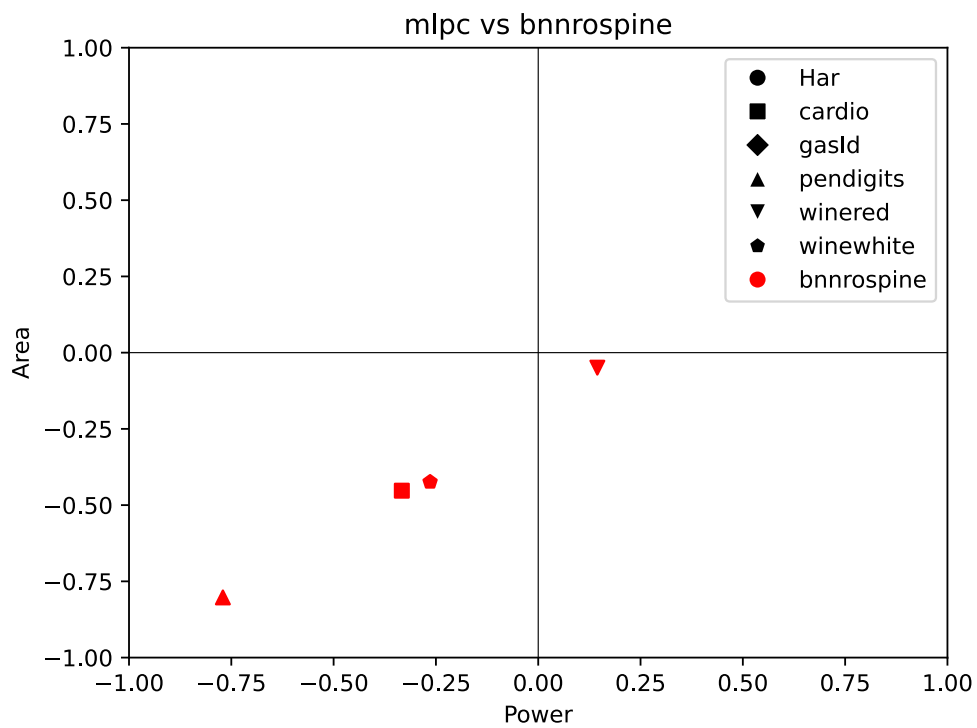|	mlpc area(cm²)	bnnrospine area(cm²)	area change	mlpc power(mW)	bnnrospine power(mW)	power change
cardio	17	9.3	-45.3%	54	36	-33.3%
pendigits	46	9.08	-80.3%	153	35.1	-77.1%
winered	8	7.61	-4.9%	27	30.9	+14.4%
winewhite	13	7.49	-42.4%	42	30.9	-26.4%

Figure 29: mlpc_bnnrospine
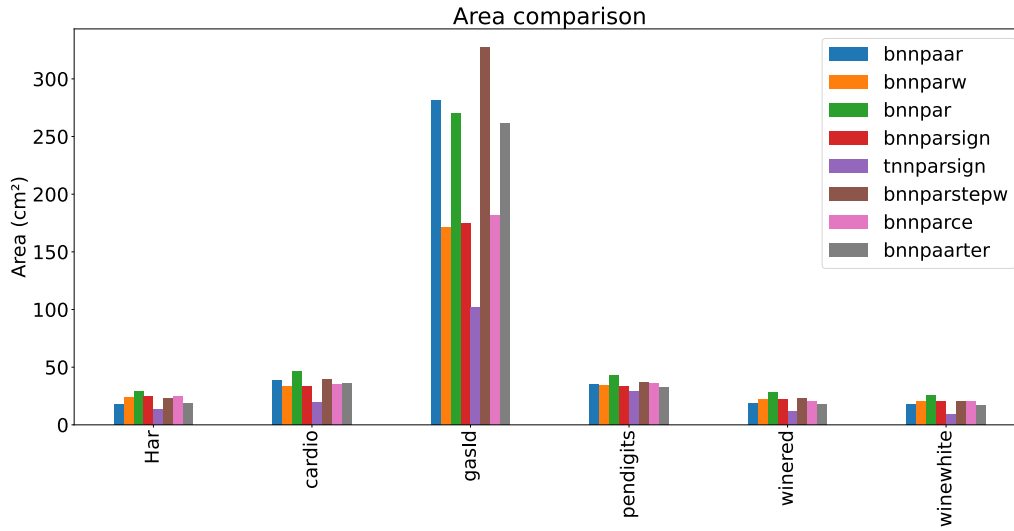
6.3   Combinatorial designs area comparisons

Table 14: What

	Har	cardio	gasId	pendigits	winered	winewhite
bnnpaar	17.42	38.74	281.55	35.43	18.55	18.01
bnnparw	24.25	33.21	171.37	33.97	21.87	20.36
bnnpar	29.4	46.71	269.76	42.95	27.82	26.01
bnnparsign	24.52	33.27	175.09	33.38	22.45	20.47
tnnparsign	13.4	19.21	101.65	29.43	11.78	9.53
bnnparstepw	23.16	39.29	326.98	37.09	22.78	20
bnnparce	24.99	34.84	181.82	35.74	20.76	20.48
bnnpaarter	18.73	35.97	261.38	32.22	17.47	16.65

6.4 Combinatorial designs power comparisons
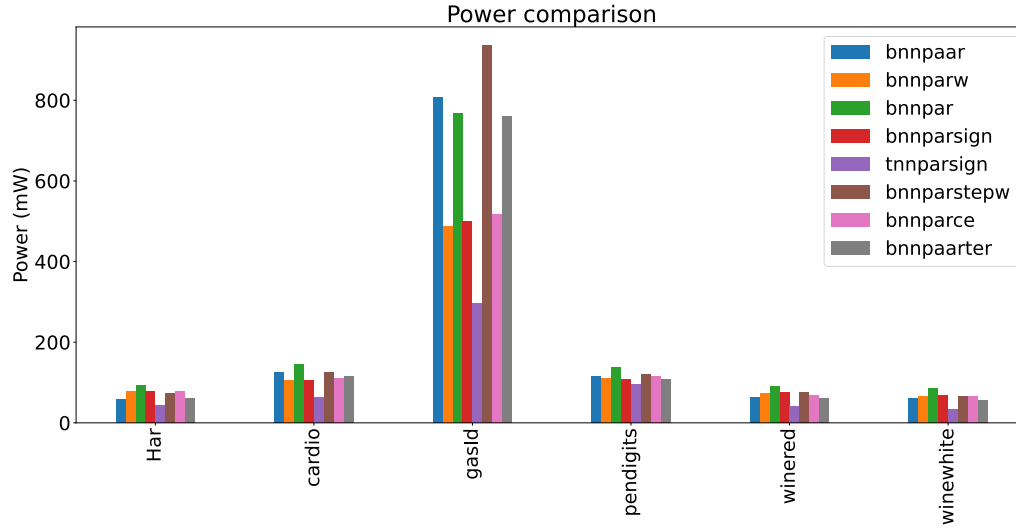
	Har	cardio	gasId	pendigits	winered	winewhite
bnnpaar	57.2	124.1	807.6	114.6	62.6	59.8
bnnparw	77.6	105.4	486.9	109.6	72.3	66.7
bnnpar	92.1	145.3	767.7	136.8	90.7	84.6
bnnparsign	78.8	106.2	499.1	108.9	74.6	68
tnnparsign	42.7	62.4	297.1	95.8	40	32.8
bnnparstepw	73.7	125.5	935.2	120.3	75.3	65.8
bnnparce	79	110.5	516.1	115.5	67.7	65.8
bnnpaarter	60.8	116	759.7	107.3	59.6	55.9

6.5   Sequential designs area comparisons
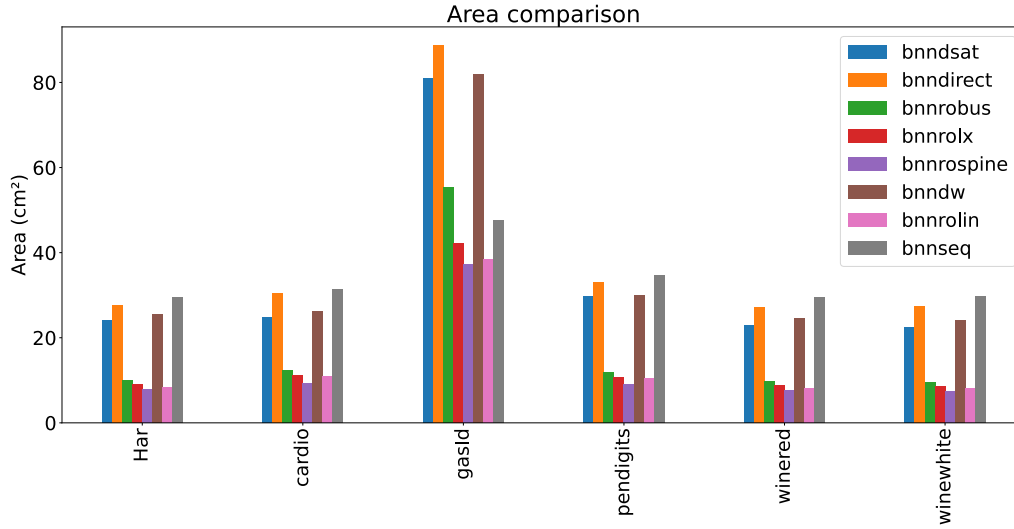
	Har	cardio	gasId	pendigits	winered	winewhite
bnndsat	24.02	24.77	81.05	29.79	23.02	22.43
bnndirect	27.63	30.5	88.62	32.93	27.11	27.31
bnnrobus	9.97	12.44	55.39	11.93	9.66	9.56
bnnrolx	9.14	11.1	42.12	10.69	8.85	8.65
bnnrospine	7.82	9.3	37.31	9.08	7.61	7.49
bnndw	25.39	26.26	81.87	29.9	24.51	23.98
bnnrolin	8.29	10.85	38.54	10.37	8.04	8
bnnseq	29.55	31.47	47.67	34.71	29.57	29.75

6.6 Sequential designs power comparisons
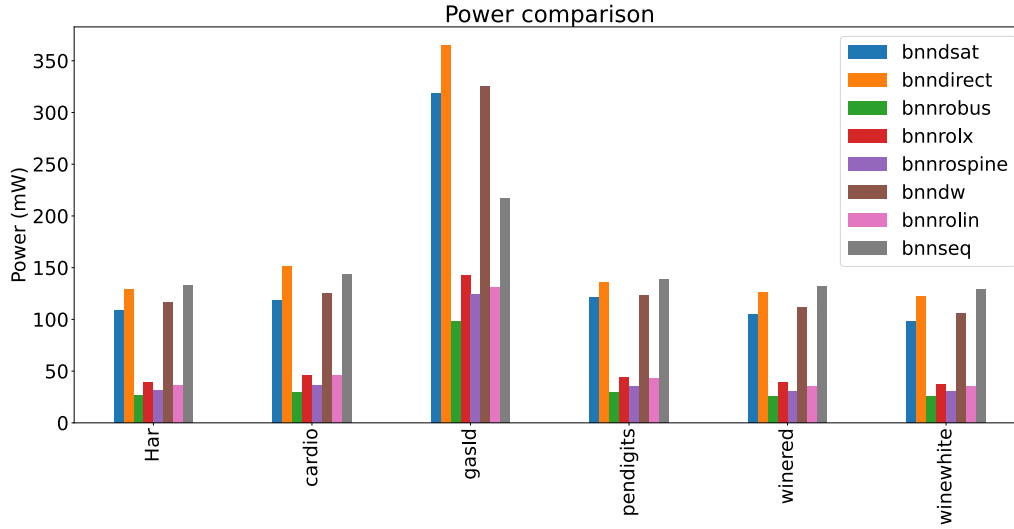
	Har	cardio	gasId	pendigits	winered	winewhite
bnndsat	109.2	118.7	318.9	121.6	104.5	98.5
bnndirect	128.8	150.8	364.5	135.7	125.7	122.6
bnnrobus	26.1	29.4	97.9	29.7	25.7	25.2
bnnrolx	39	45.5	142.4	43.5	38.9	37.5
bnnrospine	31.7	36	124.4	35.1	30.9	30.9
bnndw	116.4	124.9	325.6	123.1	112.1	106.2
bnnrolin	36.3	45.6	131.3	42.6	35.7	34.9
bnnseq	132.7	143.1	216.8	139	131.7	128.6

6.7   Additional table comparisons

Table 18: Effect of using a custom multiplexer per neuron in the first layer

	bnnseq area(cm²)	bnndirect area(cm²)	area change	bnnseq power(mW)	bnndirect power(mW)	power change
Har	29.55	27.63	-6.5%	132.7	128.8	-2.9%
cardio	31.47	30.5	-3.1%	143.1	150.8	+5.4%
gasId	47.67	88.62	+85.9%	216.8	364.5	+68.1%
pendigits	34.71	32.93	-5.1%	139	135.7	-2.4%
winered	29.57	27.11	-8.3%	131.7	125.7	-4.6%
winewhite	29.75	27.31	-8.2%	128.6	122.6	-4.7%

Table 19: Effect of reducing the width of the first layer's registers

	bnndirect area(cm²)	bnndw area(cm²)	area change	bnndirect power(mW)	bnndw power(mW)	power change
Har	27.63	25.39	-8.1%	128.8	116.4	-9.6%
cardio	30.5	26.26	-13.9%	150.8	124.9	-17.2%
gasId	88.62	81.87	-7.6%	364.5	325.6	-10.7%
pendigits	32.93	29.9	-9.2%	135.7	123.1	-9.3%
winered	27.11	24.51	-9.6%	125.7	112.1	-10.8%
winewhite	27.31	23.98	-12.2%	122.6	106.2	-13.4%

Table 20: Effect of applying saturation to the first layer's registers

	bnndw area(cm²)	bnndsat area(cm²)	area change	bnndw power(mW)	bnndsat power(mW)	power change
Har	25.39	24.02	-5.4%	116.4	109.2	-6.2%
cardio	26.26	24.77	-5.7%	124.9	118.7	-5.0%
gasId	81.87	81.05	-1.0%	325.6	318.9	-2.1%
pendigits	29.9	29.79	-0.4%	123.1	121.6	-1.2%
winered	24.51	23.02	-6.1%	112.1	104.5	-6.8%

	bnndw area(cm²)	bnndsat area(cm²)	area change	bnndw power(mW)	bnndsat power(mW)	power change
winewhite	23.98	22.43	-6.5%	106.2	98.5	-7.3%

Table 21: Effect of deconstructing negation

	bnnrolx area(cm²)	bnnrolin area(cm²)	area change	bnnrolx power(mW)	bnnrolin power(mW)	power change
Har	9.14	8.29	-9.3%	39	36.3	-6.9%
cardio	11.1	10.85	-2.3%	45.5	45.6	+0.2%
gasId	42.12	38.54	-8.5%	142.4	131.3	-7.8%
pendigits	10.69	10.37	-3.0%	43.5	42.6	-2.1%
winered	8.85	8.04	-9.2%	38.9	35.7	-8.2%
winewhite	8.65	8	-7.5%	37.5	34.9	-6.9%

Table 22: Effect of replacing the cycle counter with shifting registers

	bnnrolin area(cm²)	bnnrospine area(cm²)	area change	bnnrolin power(mW)	bnnrospine power(mW)	power change
Har	8.29	7.82	-5.7%	36.3	31.7	-12.7%
cardio	10.85	9.3	-14.3%	45.6	36	-21.1%
gasId	38.54	37.31	-3.2%	131.3	124.4	-5.3%
pendigits	10.37	9.08	-12.4%	42.6	35.1	-17.6%
winered	8.04	7.61	-5.3%	35.7	30.9	-13.4%
winewhite	8	7.49	-6.4%	34.9	30.9	-11.5%

Table 23: Effect of using tristate buffers for the weight memory

	bnnrospine area(cm²)	bnnrobus area(cm²)	area change	bnnrospine power(mW)	bnnrobus power(mW)	power change
Har	7.82	9.97	+27.5%	31.7	26.1	-17.7%
cardio	9.3	12.44	+33.8%	36	29.4	-18.3%
gasId	37.31	55.39	+48.5%	124.4	97.9	-21.3%
pendigits	9.08	11.93	+31.4%	35.1	29.7	-15.4%
winered	7.61	9.66	+26.9%	30.9	25.7	-16.8%
winewhite	7.49	9.56	+27.6%	30.9	25.2	-18.4%

6.8 Additional graph comparisons

The following graphs show the area and power measurements of the models reified via the second design normalised on the equivalent metrics from the first design type.
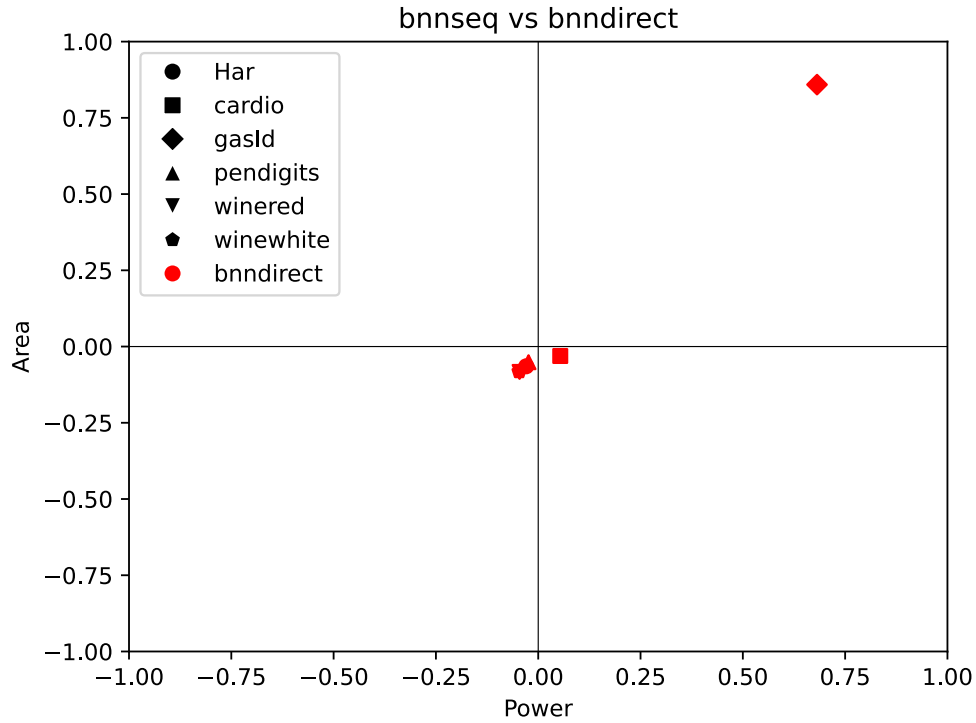

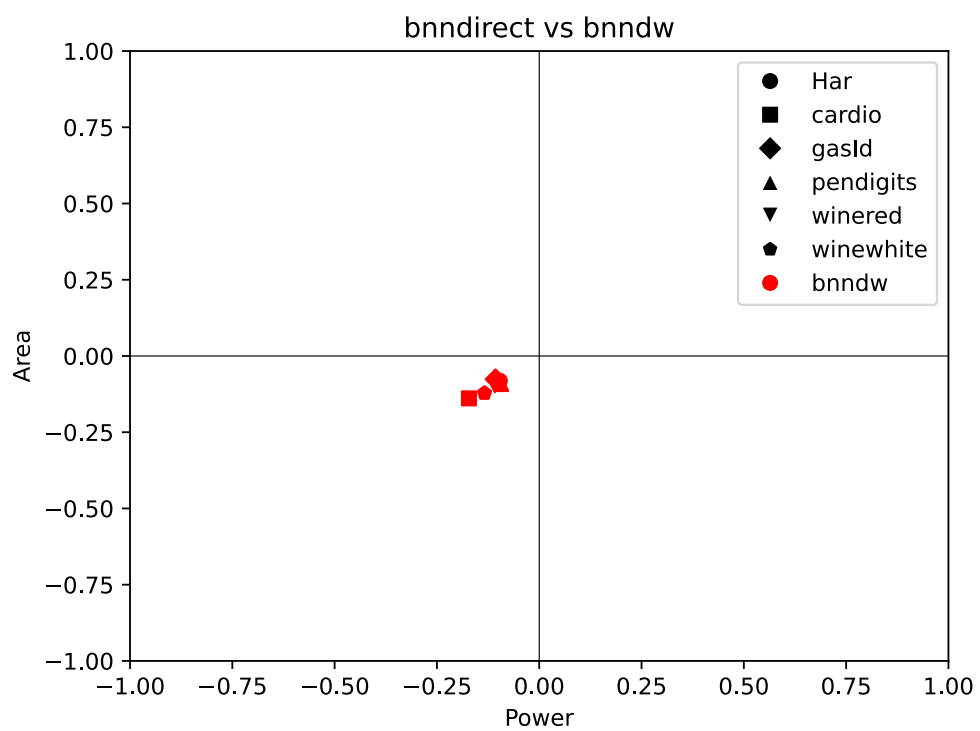Figure 30: Effect of using a custom multiplexer per neuron in the first layer

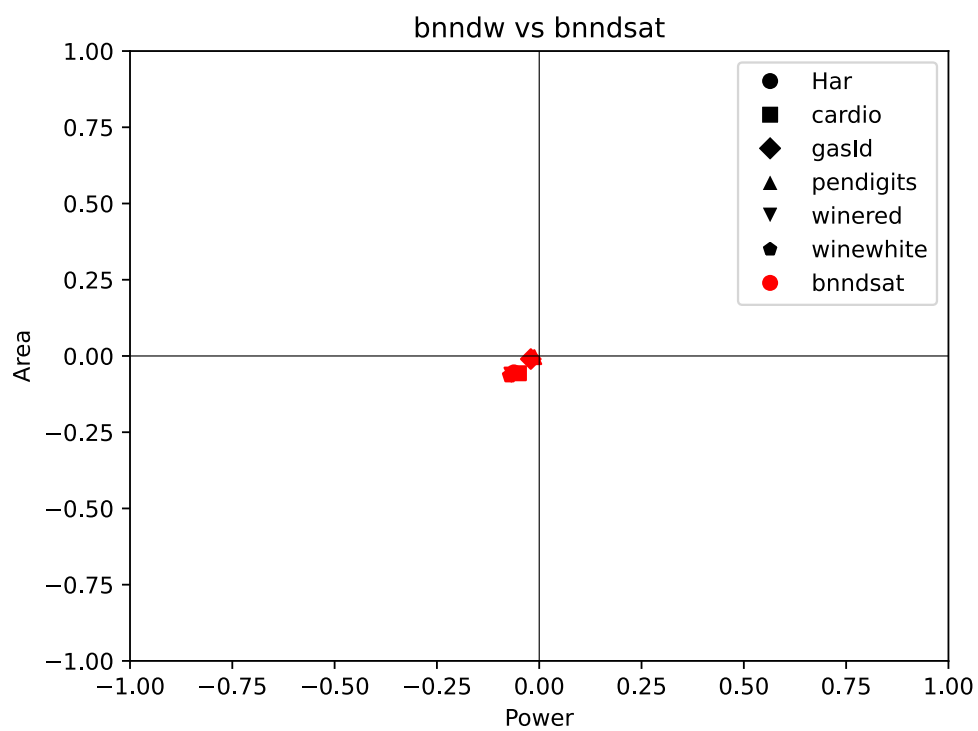Figure 31: Effect of reducing the width of the first layer's registers

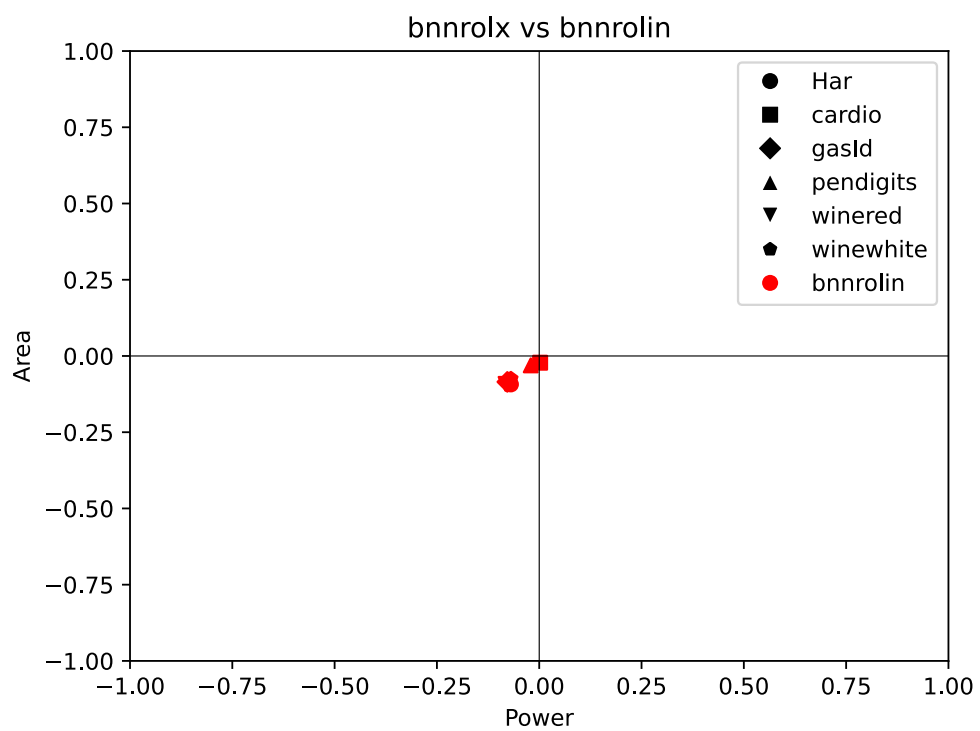Figure 32: Effect of applying saturation to the first layer's registers

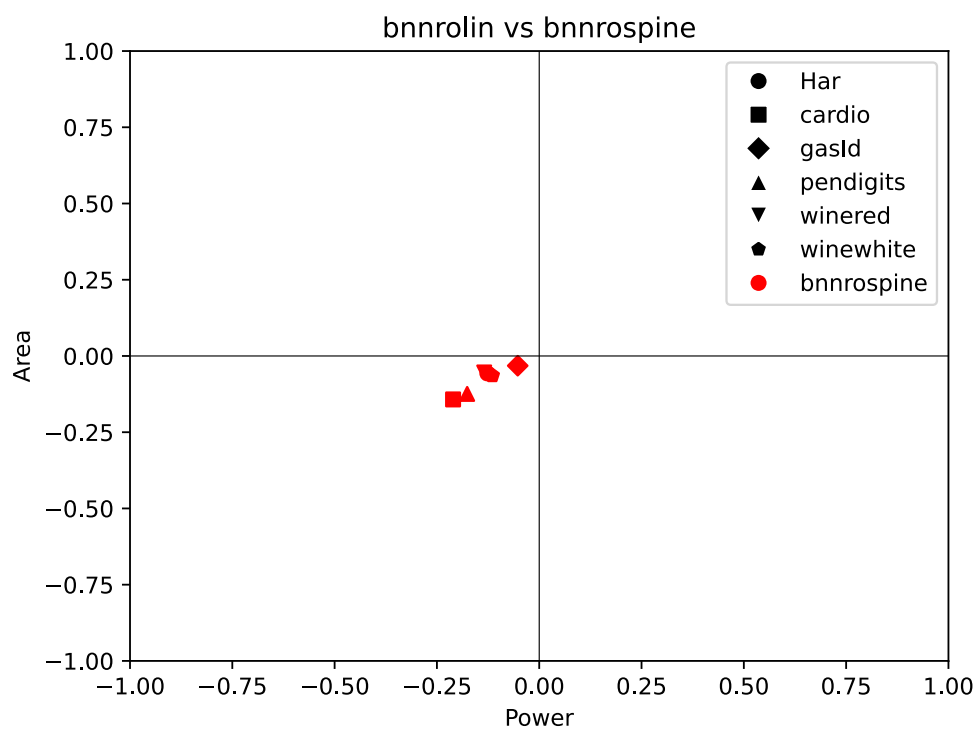Figure 33: Effect of deconstructing negation

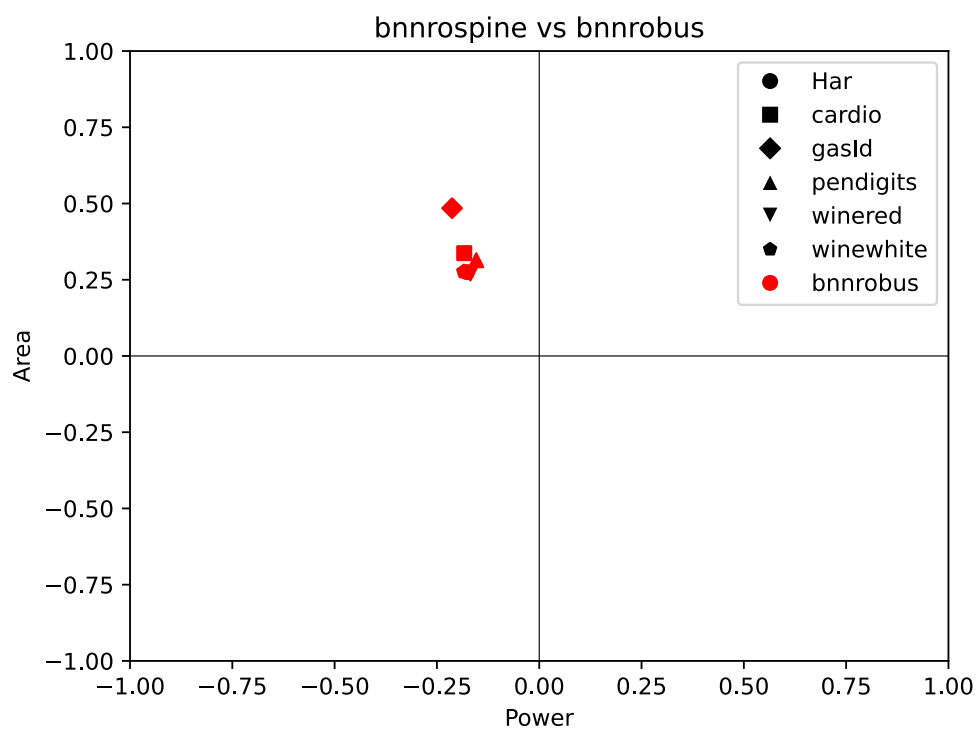Figure 34: Effect of replacing the cycle counter with shifting registers

Figure 35: Effect of using tristate buffers for the weight memory